Published by Institute of Physics Publishing for SISSA

Received: *July 8, 2008*
Accepted: *August 27, 2008*
Published: *September 4, 2008*

Real mirror symmetry for one-parameter hypersurfaces

Daniel Krefl

Arnold Sommerfeld Center for Theoretical Physics, LMU, Munich, Germany, and
PH-TH Division, CERN, Geneva, Switzerland
E-mail: krefl@mail.cern.ch

Johannes Walcher*

Institute for Theoretical Physics, ETH Zurich, Switzerland
E-mail: walcher@ias.edu

Abstract: We study open string mirror symmetry for one-parameter Calabi-Yau hypersurfaces in weighted projective space. We identify mirror pairs of D-brane configurations, derive the corresponding inhomogeneous Picard-Fuchs equations, and solve for the domainwall tensions as analytic functions over moduli space. Our calculations exemplify several features that had not been seen in previous work on the quintic or local Calabi-Yau manifolds. We comment on the calculation of loop amplitudes.

Keywords: Topological Strings, D-branes.

JHEP09(2008)031

*On leave from: Institute for Advanced Study, Princeton, NJ, U.S.A.

Contents

JHEP09(2008)031

1. Introduction and overview

The purpose of this paper is to extend recent progress in open string mirror symmetry for the quintic [1, 2] to the class of Calabi-Yau hypersurfaces, X, in weighted projective space, with one-dimensional Kähler moduli space, i.e., $h_{11}(X) = 1 = h_{21}(Y)$, where Y is the mirror manifold of X.

There are three models of this type (excluding the quintic), characterized by the five positive integer weights $(\nu_1, \ldots, \nu_5)$, such that $k := \sum \nu_i$ is divisible by each of the ν_i (Gepner models), and all five mutually coprime. We will denote $k/\nu_i =: h_i$. These models were considered in the early days of mirror symmetry [3 – 5] as the simplest class of examples to which to extend the original computation of Candelas et al. [6] on the quintic.

The manifolds of the A-model, $X^{(k)}$, are hypersurfaces of degree k in weighted projective space $\mathbb{P}^4(\nu_1,\ldots,\nu_5)$:

$$\begin{aligned} X^{(6)} &\subset \mathbb{P}^4(1,1,1,1,2)\,, \\ X^{(8)} &\subset \mathbb{P}^4(1,1,1,1,4)\,, \\ X^{(10)} &\subset \mathbb{P}^4(1,1,1,5,2)\ . \end{aligned} \tag{1.1}$$

The corresponding mirror manifolds, $Y^{(k)}$, are resolutions of quotients of specific one-parameter families of degree k hypersurfaces by the group $G = \hat{G}/\mathbb{Z}_k$, where $\hat{G} = \mathrm{Ker}\big(\prod_i \mathbb{Z}_{h_i} \to \mathbb{Z}_k\big)$ is the Greene-Plesser orbifold group.

$$\begin{aligned} Y^{(6)}: &\qquad \frac{1}{6}\left(x_1^6+x_2^6+x_3^6+x_4^6+2x_5^3\right) - \psi x_1x_2x_3x_4x_5 = 0\,, \\ Y^{(8)}: &\qquad \frac{1}{8}\left(x_1^8+x_2^8+x_3^8+x_4^8+4x_5^2\right) - \psi x_1x_2x_3x_4x_5 = 0\,, \\ Y^{(10)}: &\qquad \frac{1}{10}\left(x_1^{10}+x_2^{10}+x_3^{10}+2x_4^5+5x_5^2\right) - \psi x_1x_2x_3x_4x_5 = 0\ . \end{aligned} \tag{1.2}$$

For compact Calabi-Yau manifolds, the only systematic construction of D-branes of the A-model (Lagrangian submanifolds) is as the fixed point set of an anti-holomorphic involution for some choice of complex structure on $X^{(k)}$. The Fermat point $\sum x_i^{h_i} = 0$ in complex structure moduli space is the most convenient for comparison with boundary conformal field theory and derivation of the mirror configurations (see below). For $X^{(6)}$ and $X^{(10)}$, the Lagrangians and their worldvolume theories are qualitatively very similar to those on the quintic, see section 2. For $X^{(8)}$, we find that for certain choices of anti-holomorphic involution, the fixed point set consists of *disconnected components* in the *same homology class*. As a consequence, the worldvolume theory has vacua corresponding to wrapping on different Lagrangian submanifolds that cannot be continuously connected through Lagrangian families. In this case, the tension of BPS domainwalls between the vacua receives corrections from both *open and closed* string worldsheet instantons. Only when all effects are combined do we obtain a physically sensible domainwall spectrum. Although this phenomenon is not unexpected in general, it had not been seen previously in explicit examples on either the quintic or local Calabi-Yau manifolds.

On the mirror side, the most convenient (and complete) description of B-type D-branes on $Y^{(k)}$ is as graded, $\hat{G}$-equivariant matrix factorizations of the hypersurface polynomial, $W^{(k)}$, viewed as Landau-Ginzburg superpotential [7]. The basic algorithm for working out the configurations mirror to the real slices of $X^{(k)}$ is described in [8]. We will follow this procedure and match the vacuum structure with that seen in the A-model.

For certain other choices of anti-holomorphic involution, also on $X^{(8)}$, the Lagrangian submanifold has a non-zero first Betti number, and hence a classical deformation space. It is of interest to ask whether this moduli space is lifted by quantum effects (worldsheet instantons). We cannot at the moment answer this question from A-model considerations. However, if our mirror proposal is correct, the B-model results indicate that this moduli space in fact persists at the quantum level, i.e., no superpotential is generated for the corresponding chiral field.

JHEP09(2008)031

We then turn in section 3 to the computation of more refined invariant information, namely the tension of BPS domainwalls, or superpotential differences, between the various brane vacua. As explained in [2], the appropriate mathematical concept is that of a Hodge theoretic *normal function*. In the B-model, it can be represented geometrically as an integral of the holomorphic three-form over a three-chain suspended between homologically equivalent holomorphic curves. The curves representing the brane vacua of our interest can be determined algorithmically from the matrix factorization via the algebraic second Chern class. The chain integral then satisfies an inhomogeneous version of the Picard-Fuchs differential equation governing closed string mirror symmetry, with an inhomogeneous term that can be computed explicitly from the curve and the Griffiths-Dwork algorithm. This Abel-Jacobi type method developped in [2] is similar in spirit to the computations in local geometries [9 – 11].

With the inhomogeneous Picard-Fuchs equation in hand, we can then compute the fully quantum corrected domainwall tension over the entire closed string moduli space, see section 4. We will check integrality of all requisite monodromy matrices, as well as the spectrum of tensionless domainwalls, expected from the matrix factorization considerations. By expanding around large complex structure/large volume, we obtain numerical predictions for the number of disks ending on the Lagrangians of the A-model, consistent with Ooguri-Vafa integrality [12].

In the final section 5, we will (before concluding) briefly discuss the computation of loop amplitudes in topological string backgrounds that include the D-branes we have studied. These computations, the details of which we leave for the future, use the extension [13, 14] of the BCOV holomorphic anomaly equations [15, 16], and yield further numerical predictions as well as additional consistency checks. Again, the most interesting example is $X^{(8)}$, where the disconnected fixed point set (as orientifold plane) allows for a variety of tadpole cancelling D-brane configurations.

2. D-brane configurations

The Fermat polynomial defining the A-model

$$\sum_{i=1}^{5} x_i^{h_i} = 0\,, \tag{2.1}$$

where $h_i := k/\nu_i$, is invariant under anti-holomorphic involutions acting as

$$x_i \to \phi_i^{M_i} \bar{x}_i\,, \tag{2.2}$$

where $\phi_i = e^{\frac{2\pi i \nu_i}{k}}$ are phases with ν_i the weights of the ambient weighted $\mathbb{P}^4 \supset X^{(k)}$. The M_i are integer, but the sets (M_i) and $(M_i + \nu_i)$ define the same involution by projective identification. The fixed-point loci, $L^{(k)}_{[M]}$, of the involutions (2.2) are special Lagrangian submanifolds of $X^{(k)}$, and can be parameterized explicitly by $x_i = \phi_i^{M_i/2} y_i$, with y_i real. When h_i is odd, two involutions differing only in M_i are equivalent (though not identical) under the global symmetry group $\mathbb{Z}_{h_i}$, hence the corresponding $L^{(k)}_{[M]}$ are isomorphic. When

h_i is even, we have to distinguish whether M_i is even or odd, which yields a sign in the equation determining the real locus,

$$\sum_{i=1}^{5}(-1)^{M_i}y_i^{h_i} = 0 \ . \tag{2.3}$$

Again, for h_i odd, M_i is equivalent to $M_i + 1$ by changing $y_i \to -y_i$.

2.1 $X^{(6)}$ and $X^{(10)}$ in the A-model

When at least one h_i is odd, say h_5, we can solve (2.3) uniquely over the reals for y_5, and identify

$$L^{(k)}_{[M]} \cong \{(y_1, \ldots, y_4) \neq (0,0,0,0)\}/\mathbb{R}^* \cong \mathbb{RP}^3 \ . \tag{2.4}$$

Thus,

$$L^{(6)}_{[M]} \cong \mathbb{RP}^3, \qquad L^{(10)}_{[M]} \cong \mathbb{RP}^3 \ . \tag{2.5}$$

for all M. The vacuum structure of a D-brane wrapped on $L^{(6)}_{[M]}$ or $L^{(10)}_{[M]}$ (think of a D6 or D4-brane in type IIA) is therefore very similar to the quintic [1]. In detail, since $H_1(\mathbb{RP}^3, \mathbb{Z}) = \mathbb{Z}_2$, there is a discrete choice of Wilson line on the D-brane wrapping the $\mathbb{RP}^3$ such that the worldvolume gauge theory will have two vacua, which we will parameterize by the discrete modulus $\sigma = \pm 1$. A BPS domainwall separating the two vacua can be obtained by wrapping a (D4 or D2-) brane on a holomorphic disk in $X^{(k)}$ with boundary on the non-trivial one-cycle in $\mathbb{RP}^3$ and with the remaining dimensions located in space-time [1]. The corresponding domainwall tension, which we will denote by $\mathcal{T}_A$, is the basic holomorphic observable associated with the D-brane configuration. At large volume, $\mathcal{T}_A$ clearly scales as $\mathcal{T}_A \sim t$, where t is the Kähler modulus. There are then quantum corrections to $\mathcal{T}_A$ due to worldsheet (disk) instantons. Monodromy considerations around $\mathrm{Im}\,(t) \to +\infty$ identical to those on the quintic (which we will review momentarily) lead us to expect an expansion[1]

$$\mathcal{T}_A = \frac{t}{2} + \left(\frac{1}{4} + \frac{1}{2\pi^2}\sum_{d \text{ odd}} \tilde{n}_d q^{d/2}\right), \tag{2.6}$$

where $q \equiv \exp(2\pi i t)$ and $\tilde{n}_d$ are the open Gromov-Witten invariants counting holomorphic maps from the disk to $X^{(k)}$ with boundary on $L^{(k)}_{[M]}$.

The reasoning that leads to the classical terms $t/2 + 1/4$ in (2.6) takes into account that the corresponding domainwall not only changes the vacuum on the brane ($\sigma = \pm 1$), but also the value of the Ramond-Ramond four and six form flux, N_4 and N_6, through the corresponding cycles of the Calabi-Yau manifold. We have [1]

$$\mathcal{T}_A = \mathcal{W}_{(N_4+1,N_6;+)} - \mathcal{W}_{(N_4,N_6;-)} = t - \left[\mathcal{W}_{(N_4,N_6;-)} - \mathcal{W}_{(N_4,N_6;+)}\right] \ . \tag{2.7}$$

The second equality follows from the fact that the domainwall mediating between N_4 and $N_4 + 1$ has tension equal to t. The large volume monodromy $t \to t + 1$ acts on the vacua

[1]The basic fact is the exact sequence $H_2(X;\mathbb{Z}) \to H_2(X, L;\mathbb{Z}) \to H_1(L;\mathbb{Z})$ in which the generator of $H_2(X, L;\mathbb{Z}) \cong \mathbb{Z}$ is mapped to the non-trivial class in $H_1(L;\mathbb{Z}) \cong H^2(L;\mathbb{Z}) \cong \mathbb{Z}_2$.

JHEP09(2008)031

as follows

$$\begin{aligned}(N_4, N_6; +) &\to (N_4, N_6 + N_4; -)\,,\\ (N_4, N_6; -) &\to (N_4 + 1, N_6 + N_4; +)\ .\end{aligned} \tag{2.8}$$

It is not hard to see that (2.6) is the only form consistent with these constraints. We emphasize that the monodromy (2.8) as well as the "one-loop" correction $\frac{1}{4}$ in (2.6) have not yet been derived from first principles, i.e. couplings of D-branes to Ramond-Ramond flux.

2.2 $X^{(8)}$ in the A-model

When all h_i are even, as happens in our examples for $X^{(8)}$, the topological type of $L^{(k)}_{[M]}$ cannot be determined straightforwardly by the previous argument, and in fact strongly depends on M. The problem was studied in a different context in [17]. It is not hard to see that in the present case we have the following types

$$\begin{aligned}L_{[0,0,0,0,0]} &= \{y_1^8 + y_2^8 + y_3^8 + y_4^8 + y_5^2 = 0\} \cong \emptyset\,,\\ L_{[0,0,0,0,1]} &= \{y_1^8 + y_2^8 + y_3^8 + y_4^8 - y_5^2 = 0\} \cong \mathbb{RP}^3 \cup \mathbb{RP}^3\,,\\ L_{[0,0,0,1,0]} &= \{y_1^8 + y_2^8 + y_3^8 - y_4^8 + y_5^2 = 0\} \cong S^3\ ,\\ L_{[0,0,0,1,1]} &= \{y_1^8 + y_2^8 + y_3^8 - y_4^8 - y_5^2 = 0\} \cong (S^1 \times S^2)/\mathbb{Z}_2\,,\\ L_{[0,0,1,1,0]} &= \{y_1^8 + y_2^8 - y_3^8 - y_4^8 + y_5^2 = 0\} \cong (S^1 \times S^2)/\mathbb{Z}_2'\ .\end{aligned} \tag{2.9}$$

The distinction between the last two lines is in the action of $\mathbb{Z}_2$ on $S^1 \times S^2$. For $[M] = [0,0,0,1,1]$, it acts by an anti-podal map on S^2, and as inversion of S^1. The Lagrangian $L = L_{[0,0,0,1,1]}$ in this case can be thought of as an S^1 bundle over $\mathbb{RP}^2$, with $H_1(L;\mathbb{Z}) = \mathbb{Z}\times\mathbb{Z}_2$, and $H_2(X, L;\mathbb{Z}) = \mathbb{Z}\times\mathbb{Z}$. For $[M] = [0,0,1,1,0]$, the residual $\mathbb{Z}_2'$ acts by a half-shift on the S^1 and by inversion of the longitudinal direction on S^2. The Lagrangian in this case is an S^2 bundle over $\mathbb{RP}^1 \cong S^1$, with $H_1(L;\mathbb{Z}) = \mathbb{Z}$ and $H_2(X, L;\mathbb{Z}) = \mathbb{Z} \times \mathbb{Z}$.

In both cases, the Lagrangian contains a real one-cycle, namely the first Betti number $b_1(L) = 1$. As is well-known, this means that the $\mathcal{N} = 1$ worldvolume theory contains a chiral multiplet whose vev measures displacement of the Lagrangian away from its original position at the fixed point locus, as well as the continuous Wilson line around the corresponding one-cycle. As is equally well-known, this chiral multiplet is massless in the large volume limit, but can gain a mass by worldsheet disk instantons [18] (i.e., it could be an obstructed deformation in the mathematical langage, [19]) with boundary in the corresponding one-cycle. Using mirror symmetry, we can study the corresponding deformation problem using classical methods. Preliminary computations on the objects mirror to the above Lagrangians (see below) indicate that their modulus in fact remains massless even away from large volume [20]. It would be interesting to find evidence for this vanishing of worldsheet instanton contribution directly in the A-model.

Another interesting case is the second line in (2.9), $L_{[0,0,0,0,1]} \cong \mathbb{RP}^3 \cup \mathbb{RP}^3$. Here, $H_1(L;\mathbb{Z}) = \mathbb{Z}_2 \times \mathbb{Z}_2$, and $H_2(X, L;\mathbb{Z}) = \mathbb{Z} \times \mathbb{Z}_2$. Thus, the fixed point locus actually consists of two components that can be wrapped *independently*. As we will see below, the

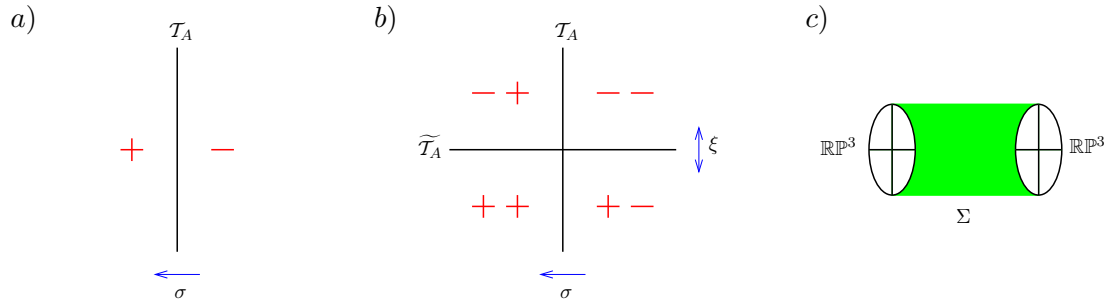

Figure 1: Illustration of the vacua of the worldvolume gauge theory of a D6-brane on a) $L^{(6)}_{[M]}$ and $L^{(10)}_{[M]}$, b) on $L^{(8)}_{[0,0,0,0,1]}$. c) Illustration of the 4-chain Σ separating the two $\mathbb{RP}^3$ components of $L^{(8)}_{[0,0,0,0,1]}$.

two components are actually homologous to each other, so that the worldvolume theory of a D-brane in this class has four vacua, labelled by the $\mathbb{RP}^3$ component it is wrapped on, and the choice of discrete Wilson line on the corresponding $\mathbb{RP}^3$. We will denote these moduli by (ξ, σ), with $\xi, \sigma = \pm 1$.

We illustrate the corresponding domainwalls in figure 1. First, we have the domainwall interpolating between the different Wilson lines on a fixed Lagrangian. For symmetry reasons, the tension does not depend which $\mathbb{RP}^3$ component we are talking about, and will be identical in structure to that on the quintic, $X^{(6)}$ and $X^{(10)}$, see (2.6). In addition, we have the possibility of interpolating between the two $\mathbb{RP}^3$'s. This is realized geometrically as a D-brane partially wrapped on an appropriate four-chain, as illustrated in figure 1c, with remaining directions extended in space-time. On dimensional grounds, the tension of this domainwall must scale as t^2 as $t \to i\infty$. In fact, one may see that by complex conjugation, we can complete the four-chain to a four-cycle, where a D6-brane wrapped on this four-cycle changes the two-form flux N_2 by one unit. The tension of this domainwall, Π_4, is nothing but the (quantum corrected) closed string period of the four-cycle. From closed string mirror symmetry [6, 4], we know that Π_4 has at large volume an expansion of the form

$$\Pi_4 = \partial_t \mathcal{F} = -\kappa \frac{t^2}{2} + at + b + \frac{1}{4\pi^2} \sum_d \tilde{N}_d d q^d \,, \tag{2.10}$$

where $\mathcal{F}$ is the genus zero prepotential. Here $\tilde{N}_d$ are the closed string Gromov-Witten invariants, κ is the classical triple intersection, and b is related to the second Chern class of the Calabi-Yau. The number a is slightly ambiguous, but can be constrained by requiring integrality of monodromy or by related considerations of D-brane charge quantization. For $X^{(8)}$, we use the values [4]

$$\kappa = 2 \,, \qquad a = -3 \,, \qquad b = \frac{11}{6} \,. \tag{2.11}$$

Thus, under large volume monodromy $t \to t + 1$,

$$\Pi_4 \to \Pi_4 + a' t + b' \,, \tag{2.12}$$

where $a' = -\kappa = -2$ and $b' = a - \frac{\kappa}{2} = -4$. We can now repeat the same steps that led to (2.6), taking into account also the 2-form flux. We find that the only way to obtain a consistent solution to the monodromy constraints is that $t \to t+1$ acts on the vacua by

$$\begin{aligned}
&(N_2, N_4, N_6; -, +) \to (N_2, N_4 + a'N_2, N_6 + N_4 + b'N_2; -, -)\,,\\
&(N_2, N_4, N_6; -, -) \to (N_2, N_4 + a'N_2 + 1, N_6 + N_4 + b'N_2; -, +)\,,\\
&(N_2, N_4, N_6; +, +) \to \left(N_2, N_4 + a'N_2 + \frac{a'}{2}, N_6 + N_4 + b'N_2 + \frac{b'}{2}; +, -\right),\\
&(N_2, N_4, N_6; +, -) \to \left(N_2, N_4 + a'N_2 + \frac{a'}{2} + 1, N_6 + N_4 + b'N_2 + \frac{b'}{2}; +, +\right),
\end{aligned} \tag{2.13}$$

and that with

$$\begin{aligned}
\mathcal{T}_A &= \mathcal{W}_{(N_2,N_4+1,N_6;\xi,+)} - \mathcal{W}_{(N_2,N_4,N_6;\xi,-)}\\
&= t - \big(\mathcal{W}_{(N_2,N_4,N_6;\xi,-)} - \mathcal{W}_{(N_2,N_4,N_6;\xi,+)}\big)\,,\\
\widetilde{\mathcal{T}_A} &= \mathcal{W}_{(N_2+1,N_4,N_6;-,\sigma)} - \mathcal{W}_{(N_2,N_4,N_6;+,\sigma)}\\
&= \Pi_4 - \big(\mathcal{W}_{(N_2,N_4,N_6;+,\sigma)} - \mathcal{W}_{(N_2,N_4,N_6;-,\sigma)}\big)\,,
\end{aligned} \tag{2.14}$$

we must have an expansion of the form (2.6) for $\mathcal{T}_A$ and

$$\widetilde{\mathcal{T}_A} = \frac{\Pi_4}{2}\,, \tag{2.15}$$

with no further corrections. Note that the existence of a solution, and in particular the integrality of the monodromy of $\widetilde{\mathcal{T}_A}$ depends on the fact that a' and b' are even integers. In section 4, we will check that the monodromies around the other singular points in moduli space are also integral.

2.3 Comparison with B-model

At the Fermat point $\psi = 0$, the polynomials in (1.2), viewed as Landau-Ginzburg potentials, $W = W^{(k)}$, admit the following set of matrix factorizations

$$Q = \sum_{i=1}^{5} \frac{1}{\sqrt{h_i}} \big(x_i^{l_i}\eta_i + x_i^{h_i - l_i}\bar{\eta}_i\big)\,, \tag{2.16}$$

where $\{\eta_i, \bar{\eta}_j\} = \delta_{ij}$ are matrices representing a Clifford algebra, and $0 < l_i < h_i$ are a set of integer parameters. Namely,

$$\big(Q\big)^2 = \sum x_i^{h_i}/h_i = W|_{\psi=0}\ . \tag{2.17}$$

The factorizations in (2.16) provide the Landau-Ginzburg description of the so-called Cardy or Recknagel-Schomerus boundary states [21] of the associated Gepner model. More precisely, we are interested in B-branes in the mirror model, which involves an orbifold of (1.2) by the Greene-Plesser orbifold group $\hat{G} = \mathrm{Ker}\big(\prod \mathbb{Z}_{h_i} \to \mathbb{Z}_k\big)$. This means that we have to equip the linear space underlying Q with an action of $\hat{G}$ such that Q is equivariant with respect to the action of $\hat{G}$ on the x_i.

JHEP09(2008)031

As shown in [8], the boundary states/matrix factorizations that provide the Landau-Ginzburg description of the real slices of the A-model hypersurfaces arise from the labels $l_i \approx h_i/2$ for $i = 1, \ldots, 5$. We will momentarily describe this correspondence. But before that, we ought to note that the factorizations (2.16) in which $l_i = h_i/2$ for all i with odd ν_i ($\equiv k/h_i$) are *reducible*. This is because

$$A = \prod_{i,\nu_i \text{ odd}} (\eta_i - \bar{\eta}_i)\,, \tag{2.18}$$

is a non-trivial degree zero element of the cohomology of Q, of square $A^2 \sim \mathrm{id}$. As first discussed in the Gepner model context in [22, 23], we can then split Q into the eigenspaces of A, as in

$$Q^{\pm} = P^{\pm} Q P^{\pm}\,, \tag{2.19}$$

where $P^{\pm} \sim \frac{1\pm A}{2}$. We will denote the elementary matrix factorization, equipped with the corresponding representation of $\hat{G}$, by

$$Q^{\zeta}_{[\mathbf{m}]}\,, \tag{2.20}$$

where $[\mathbf{m}] \in \big(\hat{G}\big)^* = \big(\prod \mathbb{Z}_{h_i}\big)/\mathbb{Z}_k$, and $\zeta = \pm 1$ is the eigenvalue of A.

The correspondence derived in [8] is that the real slice $L^{(k)}_{[M]}$ of an *even-degree* hypersurface with respect to the involution (2.2), is represented, *at the level of topological charges*, by the following linear combination of tensor product states:

$$\big[L_{[M]}\big] = \frac{1}{2}\big[Q_{[\mathbf{m}^+]}\big] - \frac{1}{2}\big[Q_{[\mathbf{m}^-]}\big]\ . \tag{2.21}$$

Here $\mathbf{m}^{\pm} = (m_1^{\pm}, \ldots, m_5^{\pm})$, and the $m_i^{\pm}$ are related to the M_i as follows: For M_i even, $m_i^+ = m_i^- = M_i/2$, and for M_i odd, $m_i^{\pm} = (m_i \pm 1)/2$. The l_i labels (*cf.*, (2.16)) are determined as follows: For h_i even, $l_i = h_i/2$. For h_i odd, and M_i even, $l_i = (h_i - 1)/2$ in the first summand, and $l_i = (h_i + 1)/2$ in the second summand. For h_i odd, and M_i odd, $l_i = (h_i + 1)/2$ in the first summand, and $l_i = (h_i - 1)/2$ in the second summand.

The relation (2.21) was obtained in [8] by comparing, via the gauged linear sigma model, the topological charges of *orientifold planes* associated with A-type parity and complex conjugation (2.2) in large volume and in the Landau-Ginzburg phase. Our goal in this paper is however to obtain more refined information than just the topological charges, for which we need to lift (2.21) (at least) to the holomorphic sector. We have no principled way of doing this at the moment, however in certain cases we can make a plausible proposal based on the following set of observations.[2]

At large volume, the fixed point set of the anti-holomorphic involution is a *special* Lagrangian submanifold, i.e., it is conformally invariant (in one-loop sigma-model expansion) and preserves space-time supersymmetry, in addition to preserving A-type worldsheet supersymmetry. An equivalent statement should hold at the Landau-Ginzburg point, since

[2]For *odd degree* hypersurfaces, such as the quintic, we have only one term on the r.h.s. of (2.21). The lift to the holomorphic sector is then more natural, and supported by a lot of evidence.

JHEP09(2008)031

to get there we only need to vary the Kähler moduli. In general, the ($\mathcal{N}=1$) spacetime supersymmetry preserved by an equivariant matrix factorization $Q_{[\mathbf{m}]}$ can be measured by the phase of the ($\mathcal{N}=2$) central charge, which (for fixed l_i) varies $\propto \sum_{i=1}^{5} \frac{m_i}{h_i}$. It is not hard to see that in most cases, the two summands in (2.21) in general preserve different supersymmetry. This means that the supersymmetric D-brane corresponding to the real hypersurface must in general be some bound state of the above components.

Let us illustrate this for the real slices of $X^{(8)}$. Evaluating (2.21) (and taking into account that the irreducible factorizations from (2.20) have the same topological charges) gives (*cf.*, (2.9)),

Langrangian	topology	matrix factorizations
$L_{[0,0,0,0,0]}$	$\emptyset$	$\left[Q^+_{[0,0,0,0,0]}\right] - \left[Q^+_{[0,0,0,0,0]}\right] = 0$
$L_{[0,0,0,0,1]}$	$\mathbb{RP}^3 \cup \mathbb{RP}^3$	$\left[Q_{[0,0,0,0,0]}\right] = \left[Q^+_{[0,0,0,0,0]}\right] + \left[Q^-_{[0,0,0,0,0]}\right]$
$L_{[0,0,0,1,0]}$	S^3	$\left[Q^+_{[0,0,0,0,0]}\right] - \left[Q^+_{[0,1,0,0,0]}\right]$
$L_{[0,0,0,1,1]}$	$(S^1 \times S^2)/\mathbb{Z}_2$	$\left[Q^+_{[0,0,0,0,0]}\right] + \left[Q^+_{[0,1,0,0,0]}\right]$
$L_{[0,0,1,1,0]}$	$(S^1 \times S^2)/\mathbb{Z}_2'$	$\left[Q^+_{[0,0,0,0,0]}\right] - \left[Q^+_{[0,1,1,0,0]}\right]$

(2.22)

The first two lines are very obvious cases: $L_{[0,0,0,0,0]}$ is empty, with vanishing boundary state. $L_{[0,0,0,0,1]}$ geometrically splits into two $\mathbb{RP}^3$ components, which we might tentatively identify with $Q^+_{[0,0,0,0,0]}$ and $Q^-_{[0,0,0,0,0]}$. (The correct dictionary must ultimately include the Wilson line degree of freedom, and is somewhat different, see eq. (4.33).) We propose that this identification holds at the holomorphic level, and probably also at the level of superconformal boundary states.

The situation for the other real slices (including those of $X^{(6)}$ and $X^{(10)}$) is less clear cut. As mentioned above, the Lagrangians can at best correspond to a bound state of the two components in (2.21), and at worst might not be continuously connected to the split form of (2.22). Nevertheless, our present observations and the calculations in the following sections suggest that the correspondence (2.22) can indeed be lifted to the holomorphic level.

To study this additional evidence, we need to present the deformation theory of the matrix factorizations Q of (2.16) with $l_i = [h_i/2]$ as we vary the complex structure parameter away from $\psi = 0$. This is a rather straightforward exercise.

For $Y^{(6)}$, we find that Q deforms in a unique way (up to gauge transformation), given explicitly by

$$Q(\psi) = \sum \frac{1}{\sqrt{6}}\left(x_i^3\eta_i + x_i^3\bar{\eta}_i\right) + \frac{1}{\sqrt{3}}\left(x_5\eta_5 + x_5^2\bar{\eta}_5\right) - \sqrt{3}\psi x_1x_2x_3x_4\bar{\eta}_5 \ . \tag{2.23}$$

This deformation commutes with A from (2.18). Therefore, by splitting as in (2.20), we obtain two families $Q^\zeta(\psi)$ (with $\zeta = \pm 1$) of matrix factorizations. We expect that the $\mathbb{RP}^3$ special Lagrangians should correspond to an appropriate bound state of those with different $[\mathbf{m}]$ label, but identical ζ-label. The latter should correspond to the discrete Wilson line on $\mathbb{RP}^3$. Hence, we identify

$$\sigma = \zeta \ . \tag{2.24}$$

For $Y^{(8)}$, we find two *inequivalent* ways of deforming the factorization away from $\psi = 0$. We will denote those matrix factorizations as $Q(\psi, \mu)$, where the additional label $\mu = \pm 1$:

$$\begin{aligned} Q(\psi,+) &= \sum \frac{1}{\sqrt{8}}\big(x_i^4\eta_i + x_i^4\bar{\eta}_i\big) + \frac{1}{\sqrt{2}}\big((x_5\eta_5 + x_5\bar{\eta}_5\big) - \sqrt{2}\psi x_1x_2x_3x_4\eta_5\,, \\ Q(\psi,-) &= \sum \frac{1}{\sqrt{8}}\big(x_i^4\eta_i + x_i^4\bar{\eta}_i\big) + \frac{1}{\sqrt{2}}\big((x_5\eta_5 + x_5\bar{\eta}_5\big) - \sqrt{2}\psi x_1x_2x_3x_4\bar{\eta}_5\,. \end{aligned} \tag{2.25}$$

Again, the deformation commutes with A. For $L_{[0,0,0,0,1]}$, this means that we obtain in total *four* families of matrix factorizations, naturally organized in two sets of two. Namely, we mind to the labels $\langle \mu, \zeta \rangle$, where ζ is the eigenvalue of A, and μ distinguishes the two lines in (2.25). We propose that those correspond to the four vacua that we identified in subsection 2.2 above. We emphasize at this stage that we still allow for a non-trivial transformation between the discrete A-model labels (ξ, σ) and the B-model labels $\langle \mu, \zeta \rangle$. We will determine this transformation after analytic continuation of domainwall tensions in section 4.

For $L_{[0,0,0,1,1]} \cong (S^1 \times S^2)/\mathbb{Z}_2$, we propose to identify the $\mu = \pm 1$ label from (2.25) with the two vacua associated with the discrete $\mathbb{Z}_2$ factor in $H_1(L_{[0,0,0,1,1]}) = \mathbb{Z} \times \mathbb{Z}_2$ (see paragraph below (2.9)). (The free factor in $H_1(L)$ (for $L = L_{[0,0,0,1,1]}$ and $L_{[0,0,1,1,0]}$) is associated at large volume with a continuous modulus, displacing the Lagrangian away from the fixed locus of the anti-holomorphic involution. As mentioned above, there are indications [20] that this open string modulus is in fact unobstructed, so should decouple from the superpotential computations.)

As on the quintic [1, 24], the two-fold way of deforming away from $\psi = 0$ is accompagnied by the appearance, at $\psi = 0$, of an additional massless field in the open string spectrum. Also, the tension of the domainwall between the $\langle +, \zeta \rangle$ and the $\langle -, \zeta \rangle$ vacua should vanish at $\psi = 0$. This will be our way to complete the identification of the four vacua in A- and B-model.

Finally, for $Y^{(10)}$, the situation is somewhat in between that of $Y^{(6)}$ and that of $Y^{(8)}$. The main difference to $Y^{(6)}$ is that the tensor product factorization has an infinitesimal modulus (degree 1 cohomology element) Ψ, the main difference to $Y^{(8)}$ is that Ψ satisfies $\{A, \Psi\} = 0$ instead of $[A, \Psi] = 0$, where A is from (2.18). Without delving into details, the consequence is that the factorizations $Q^{\pm}$ from (2.20) deform in a unique way, which can be obtained by splitting the deformed factorization

$$\begin{aligned} Q(\psi) = \sum \frac{1}{\sqrt{10}}\big(x_i^5\eta_i + x_i^5\bar{\eta}_i\big) + \frac{1}{\sqrt{2}}\big(x_4\eta_4 + x_4\bar{\eta}_4\big) + \frac{1}{\sqrt{5}}\big(x_5^2\eta_5 + x_5^3\bar{\eta}_5\big) \\ - \frac{\psi}{\sqrt{2}}x_1x_2x_3(\eta_4 + \bar{\eta}_4)x_5 - \frac{\psi^2}{2}\sqrt{5}x_1^2x_2^2x_3^2\bar{\eta}_5\,, \end{aligned} \tag{2.26}$$

in eigenspaces of A. Again, we identify the eigenvalue of A with the discrete Wilson line on $\mathbb{RP}^3 \cong L^{(10)}_{[M]}$, as in (2.24)

Since the factorizations on $Y^{(6)}$ and $Y^{(10)}$ deform in a unique way, there is no additional massless open string, and we expect no tensionless domainwall at $\psi = 0$. We will confirm this in section 4.

Before closing this section, we note another property (valid for all three k's) of the factorizations around the Fermat point $\psi = 0$. This is a special point in moduli space in which the hypersurfaces $Y^{(k)}$ gain an additional $\mathbb{Z}_k$ automorphism multiplying one of the weight-one variables by a phase. Put differently, the *monodromy around the Gepner point* $\psi \to e^{2\pi i/k}\psi$ can be undone by rotating $x_1 \to e^{-2\pi i/k}x_1$. At the level of matrix factorizations, this monodromy has to be accompagnied by conjugating Q with a representation of the $\mathbb{Z}_k$ symmetry group of the corresponding minimal model x_1^k. It is not hard to see that the matrix A from (2.18) *picks a sign* under this symmetry. Thus, we conclude that *monodromy around the Gepner point exchanges the vacua labelled by* $\zeta = \pm 1$.[3] This is another clue that we will pick up in our monodromy discussion in section 4.

3. Inhomogeneous Picard-Fuchs equations

We now wish to determine the non-perturbative α' (disk instanton) corrections to the classical approximations to the domainwall tensions (2.6), (2.14) between the various vacua on our branes. The basic strategy is as follows.

For each A-model domainwall, we identified a (virtual linear combination of) matrix factorization Q describing the D-brane configuration in the mirror B-model. The algebraic second Chern class of this matrix factorization can be represented by a homologically trivial codimension-2 algebraic cycle C (in other words, an integral linear combination of holomorphic curves)

$$c_2(Q) = [C] \in \mathrm{CH}^2_{\mathrm{hom}}(Y)\,, \tag{3.1}$$

which we will explicitly compute from the matrix factorization. There then exists a three-chain Γ of boundary C, well-defined up to closed three-cycle $\Gamma^c \in H_3(Y;\mathbb{Z})$. The domainwall tension is computed by the integral over Γ

$$\mathcal{T}_B(z) = \int_\Gamma \hat{\Omega}(z)\,, \tag{3.2}$$

where $\hat{\Omega}(z)$ is the appropriately normalized holomorphic three-form of the B-model geometry (see below).

Explicitly, we will have relations of the form

$$\mathcal{T}_B(z(t))/\varpi_0(z(t)) = \mathcal{T}_A(t)\,, \tag{3.3}$$

where the mirror map consists of the relation $z = z(t)$ between A- and B-model variables, and the normalization of the holomorphic three-form $\hat{\Omega}(z) \to \hat{\Omega}(z)/\varpi_0(z)$. As is well-known, this data can be obtained by solving the homogenous Picard-Fuchs equation satisfied by the B-model periods. The Picard-Fuchs operators of our three models are:

$$\begin{aligned}
\mathcal{L}^{(6)} &:= \theta^4 - 2^4 3^6 z(1/6+\theta)(1/3+\theta)(2/3+\theta)(5/6+\theta)\,,\\
\mathcal{L}^{(8)} &:= \theta^4 - 2^{16} z(1/8+\theta)(3/8+\theta)(5/8+\theta)(7/8+\theta)\,,\\
\mathcal{L}^{(10)} &:= \theta^4 - 5^5 2^8 z(1/10+\theta)(3/10+\theta)(7/10+\theta)(9/10+\theta)\,,
\end{aligned} \tag{3.4}$$

[3] To complete this, note that for $Y^{(8)}$, Gepner monodromy does not affect the μ-label, as can also be seen from (2.25).

with $\theta = z\partial_z$, and $z \sim \psi^{-k}$. Namely, $\varpi_0(z)$ is the unique solution with power series behavior at $z = 0$, and if $\varpi_1(z) \sim \varpi_0(z)\log(z)$ is the solution with a single logarithm, we have

$$t(z) = \frac{\varpi_1(z)}{\varpi_0(z)} \ . \tag{3.5}$$

To calculate the chain integral in (3.2), we exploit that it satisfies an inhomogeneous version of the Picard-Fuchs equation,

$$\mathcal{L}^{(k)}\mathcal{T}_B = \frac{c^{(k)}}{16}\sqrt{z} \ . \tag{3.6}$$

The central part of our computation is the determination of the parameters $c^{(k)}$ for each of our domainwalls.

3.1 From matrix factorizations to curves

Given the matrix factorizations, we obtain the curves representing the algebraic second Chern classes by the algorithm described in [2] for the quintic. This can be viewed as an application of the homological Calabi-Yau/Landau-Ginzburg correspondence [25, 26] together with elementary methods for the computation of Chern classes. The only point on which we will be slightly less rigorous than in [2] is that we will perform our computation as if we were pretending to be working on the hypersurfaces (1.2) in weighted projective space, without orbifold. In actuality, however, everything is taking place on the B-model side, i.e., the underlying manifolds are indeed $Y^{(k)}$, *after* quotienting by $G = \hat{G}/\mathbb{Z}_k$.

After some algebra, we find that the relevant part of the second Chern classes of the matrix factorizations from eqs. (2.23), (2.25), (2.26) can be represented with the following set of curves.

$$k = 6: \qquad C^{(6)}_{\zeta} = \{x_1 + (\alpha^{(6)})^{\zeta} x_2 = 0, x_3 + \alpha^{(6)} x_4 = 0, x_5^2 - 3\psi x_1 x_2 x_3 x_4 = 0\} \tag{3.7}$$

$$k = 8: \qquad C^{(8)}_{\langle \mu,\zeta\rangle} = \begin{cases} \{x_1 + (\alpha^{(8)})^{\zeta} x_2 = 0, x_3 + \alpha^{(8)} x_4 = 0, x_5 = 0\} & \mu = +1 \\ \{x_1 + (\alpha^{(8)})^{\zeta} x_2 = 0, x_3 + \alpha^{(8)} x_4 = 0, x_5 - 2\psi x_1 x_2 x_3 x_4 = 0\} & \mu = -1 \end{cases} \tag{3.8}$$

$$k = 10: \qquad C^{(10)}_{\zeta} = \{x_1 + (\alpha^{(10)})^{\zeta} x_2 = 0, x_3^5 + (\alpha^{(10)})^5\sqrt{5}\big(x_5 - \psi x_1 x_2 x_3 x_4\big) = 0, \tag{3.9}$$

$$2x_4^3 - 5\psi^2 x_1^2 x_2^2 x_3^2 = 0\} \ . \tag{3.10}$$

Let us explain our notation and the precise meaning of those equations. First of all, $\alpha^{(k)}$ are phases which fulfill $(\alpha^{(k)})^k = -1$. One then easily checks that the curves actually lie on the corresponding hypersurface, i.e., $W^{(k)} = 0$ identically whenever a group of three equations from (3.7) are satisfied. The subscript ζ comes from the eigenvalue of A used to split the reducible Q from (2.16) in two components (for the geometric meaning of ζ, see two paragraphs below). Since the second Chern class does not depend on the representation of $\hat{G}$, we have omitted the $[\mathbf{m}]$ label.

Next, we notice that the curves in (3.7) are not invariant under the orbifold group G. Instead, G maps each curve to a similar one with different choices of k-th roots of -1 in

k	$G_{\rm fix}$	generator
6	$\mathbb{Z}_6$	$(\gamma,\gamma,\gamma^{-1},\gamma^{-1},1)$
8	$\mathbb{Z}_4$	$(\gamma,\gamma,\gamma^{-1},\gamma^{-1},1)$
10	$\mathbb{Z}_{10}$	$(\gamma,\gamma,\gamma^{8},1,1)$

Table 1: The curves from (3.7) are invariant under certain subgroup of the orbifold group G. For each k, $\gamma = \gamma_k = \exp(2\pi i/k)$.

k	$\Upsilon^{(k)}$	$\mathrm{Ord}(G^{(k)})$	$\sqrt{z}$	$\rho^{(k)}$
6	$6^{-4}\psi^{-3}$	$3\cdot 6^2$	$2\cdot 6^{-3}\psi^{-3}$	$3^2\pi^{-4}$
8	$2^{-12}\psi^{-6}$	$2\cdot 8^2$	2^{-8}	$2^3\pi^{-4}\psi^{-2}$
10	$10^{-4}\psi^{-8}$	10^2	$2^{-4}5^{-5/2}\psi^{-5}$	$4\cdot 5^{1/2}\pi^{-4}\psi^{-3}$

Table 2: Parameters used in the main text for the hypersurfaces under consideration.

the corresponding equation, and the second Chern class should be thought of as this orbit of curves in $Y^{(k)}$. However, note that in each case, a certain subgroup $G_{\rm fix} \subset G$ does leave the curve invariant. This will lead to an additional normalization factor in our calculations in the next subsection. We identify the respective subgroups in table 1.

To explain the geometric role of the parameter $\zeta = \pm 1$ in (3.7), we consider the case $k = 6$ (the discussion on the other two models is the same). The set of curves $\{x_1 + \alpha x_2 = 0, x_3 + \beta x_4 = 0, x_5^2 - 3\psi x_1 x_2 x_3 x_4 = 0\}$, where α and β are arbitrary 6-th roots of -1 all lie on $X^{(6)}$. Those curves organize into two distinct orbits under the action of $G^{(k)}$, precisely distinguished by $\zeta = \pm 1$. It is clear that the Gepner monodromy $\psi \to e^{2\pi i/k}\psi$, $x_1 \to e^{-2\pi i/k} x_1$ exchanges those two orbits, $\zeta \to -\zeta$, just as we had noted it at the end of the previous section.

3.2 From curves to Picard-Fuchs

We derive the inhomogeneous Picard-Fuchs equation, i.e., the constants $c^{(k)}$ in (3.6) by using the Griffiths-Dwork method. We give the details of the computation in the appendix, and only summarize the salient steps here.

The normalization of the holomorphic three-form for which we will quote the $c^{(k)}$ is given by

$$\hat{\Omega} = \frac{\mathrm{Ord}(G^{(k)})}{(2\pi i)^3}\psi\Omega\,, \tag{3.11}$$

where Ω is the standard residue from projective space (see below (A.2)) and the $\mathrm{Ord}(G^{(k)})$ are the orders of the groups yielding the mirror manifold. We list those together with some other normalization data in table 2. The choice (3.11) is the normalization in which the regular integral period $\varpi_0(z)$ has a unit constant term, $\varpi_0(z) = 1 + \mathcal{O}(z)$.

The implementation of the Griffiths-Dwork algorithm however is easier in a slightly different normalization of the holomorphic three-form, in which the homogeneous Picard-Fuchs operator takes the form $\tilde{\mathcal{L}}^{(k)}$ given in equations (A.7), (A.30) and (A.49). They are

related to the Picard-Fuchs operators $\mathcal{L}^{(k)}$ given in equation (3.4) by the relation

$$\mathcal{L}^{(k)} = -\Upsilon^{(k)}\tilde{\mathcal{L}}^{(k)}\frac{1}{\psi}\,, \tag{3.12}$$

where the $\Upsilon^{(k)}$ are given in table 2.

Putting the normalization together, the statement that $\mathcal{T}_B$ given in (3.2) (for a certain choice of curves and three-chain, explained momentarily) satisfies the inhomogeneous Picard-Fuchs equation given in (3.6) translates to the identity

$$\tilde{\mathcal{L}}^{(k)}\int_{T_\epsilon(\Gamma)}\tilde{\Omega} = -\frac{(2\pi i)^4}{\Upsilon^{(k)}\,\mathrm{Ord}(G^{(k)})}c^{(k)}\sqrt{z}\,, \tag{3.13}$$

where $\tilde{\Omega}$ is defined in (A.2) and where we have used (A.4). If the functional form $\propto\sqrt{z}$ is correct, the $c^{(k)}$ are the only unknown parameters, and the claim reduces to determine the constants $c^{(k)}$ in (3.13). That is, we can solve for $c^{(k)}$:

$$c^{(k)} = -\rho^{(k)}\tilde{\mathcal{L}}^{(k)}\int_{T_\epsilon(\Gamma)}\tilde{\Omega}\,, \tag{3.14}$$

where the $\rho^{(k)}$ are given in table 2.

In (3.13), $T_\epsilon(\Gamma)$ is a small tube around a three-chain suspended between the appropriate combination of curves. We are interested in the following B-model integrals (the curves are defined in (3.7)):

k	domainwall tension	curve combination
6	$\mathcal{T}_B$	$C_+^{(6)} - C_-^{(6)}$
8	$\mathcal{T}_B$	$C^{(8)}_{\langle+,+\rangle} - C^{(8)}_{\langle-,+\rangle}$
8	$\widetilde{\mathcal{T}_B}$	$C^{(8)}_{\langle+,+\rangle} - C^{(8)}_{\langle-,-\rangle}$
10	$\mathcal{T}_B$	$C_+^{(10)} - C_-^{(10)}$

(3.15)

For $k = 8$, we make the choice to denote by $\mathcal{T}_B$ the domainwall tension that vanishes at $\psi = 0$, which completely specifies the 3-chain between the respective curves. All other domainwall tensions are only define modulo integral periods for the moment.

There are in principle two types of contributions to $\tilde{\mathcal{L}}^{(k)}\int_{T_\epsilon(\Gamma)}\tilde{\Omega}$, depending on whether $\tilde{\mathcal{L}}^{(k)}$ acts on the holomorphic three-form, or on the (tube over the) three-chain. As on the quintic, it turns out that the latter contribution always vanishes (see appendix). Thus, we just need to evaluate

$$\int_{T_\epsilon(\Gamma)}\tilde{\mathcal{L}}^{(k)}\tilde{\Omega} = \int_{T_\epsilon(\partial\Gamma)}\tilde{\beta}^{(k)}\,, \tag{3.16}$$

where $\tilde{\beta}^{(k)}$ are the exact parts of the inhomogeneous Picard-Fuchs equations given in equations (A.8), (A.31) and (A.50). Thus the crucial integrals are those of $\tilde{\beta}^{(k)}$ over the tubes around the curves $C_\zeta^{(k)}$ for $k \in \{6, 10\}$ and $C_{\zeta\mu}^{(k)}$ for $k = 8$.

The main property of the curves that allows the evaluation of these integrals is their planarity. Namely, as on the quintic, the curves $C_\zeta^{(k)}$ and $C_{\zeta\mu}^{(8)}$ are components of the

intersection of the hypersurface with an appropriately chosen plane $P^{(k)}$. Except for a small neighborhood of the intersection of the components of $P^{(k)} \cap Y^{(k)}$, the tube around the curves can be laid into the plane, where the meromorphic three-form $\tilde{\beta}^{(k)}$ vanishes trivially. We give the remaining details of this calculation in the appendix. The results are the following:

$$k = 6 : \qquad \int_{T_\epsilon(C_\zeta^{(6)})} \tilde{\beta}^{(6)} = \zeta \, \frac{4}{3}\pi^2 \,, \tag{3.17}$$

$$k = 8 : \qquad \int_{T_\epsilon(C_{\zeta\mu}^{(8)})} \tilde{\beta}^{(8)} = \zeta\mu \, 3\pi^2\psi^2 \,, \tag{3.18}$$

$$k = 10 : \qquad \int_{T_\epsilon(C_\zeta^{(10)})} \tilde{\beta}^{(10)} = \zeta \, \frac{16}{5}\sqrt{5}\pi^2\psi^3 \,. \tag{3.19}$$

Referring to (3.14) and (3.15), this translates to the following values for the constants $c^{(k)}$ for each of our domainwalls:

k	domainwall	$c^{(k)}$
6	$\mathcal{T}_B$	$\frac{24}{\pi^2}$
8	$\mathcal{T}_B$	$\frac{48}{\pi^2}$
8	$\widetilde{\mathcal{T}_B}$	0
10	$\mathcal{T}_B$	$\frac{128}{\pi^2}$

(3.20)

We now proceed to the explicit solution of the inhomogeneous Picard-Fuchs equation (3.6).

4. Analytic continuation

As on the quintic [1], it turns out that the constant $c^{(k)}$ that we computed in the previous section can almost uniquely be recovered by assuming an inhomogeneous term $\sim \sqrt{z}$ and requiring integrality of monodromy around the various special points in moduli space. We will follow this route here, and connect to the previous discussion at the end. We denote by $\tau^{(k)}(z)$ the solution of the corresponding fifth order operator $(2\theta - 1)\mathcal{L}^{(k)}$ with squareroot behaviour at $z = 0$. Note that for simplicity, we will sometimes drop the $^{(k)}$ indices in the following, which quantity carries a $^{(k)}$ index should be clear from the context.

4.1 Solutions

The solutions of the Picard-Fuchs equations of our hypersurfaces around $z = 0$ can by obtained by the Frobenius method from the following hypergeometric generating function

$$\Pi^{(k)}(z; H) = \sum_{m=0}^{\infty} z^{m+H} \frac{\Gamma\big(k(m+H)+1\big)}{\prod_{i=1}^{5} \Gamma\big(\nu_i(m+H)+1\big)} \,. \tag{4.1}$$

Namely, one checks that by expanding (4.1) in powers of H,

$$\Pi^{(k)}(z; H) = \sum_{j=0}^{3} H^j \Pi_{2j}^{(k)}(z) \bmod H^4 \,, \tag{4.2}$$

the $\Pi^{(k)}_{2j}(z)$ satisfy $\mathcal{L}^{(k)}\Pi^{(k)}_{2j}(z) = 0$. Quite remarkably, the additional solution of our inhomogeneous equation can be obtained by setting $H = 1/2$ in (4.1)

$$\tau^{(k)}(z) = \Pi^{(k)}(z; 1/2) \ . \tag{4.3}$$

It satisfies

$$\mathcal{L}^{(k)}\tau^{(k)}(z) = \frac{\tilde{c}^{(k)}}{16}\sqrt{z}\,, \tag{4.4}$$

where

$$\tilde{c}^{(k)} = \frac{\Gamma\big(k/2+1\big)}{\prod\Gamma\big(\nu_i/2+1\big)} \ . \tag{4.5}$$

The radius of convergence of the series (4.3) is, as for the closed string periods, given by $|z| < R_* \equiv \prod \nu_i^{\nu_i}/k^k$. To analytically continue $\tau^{(k)}(z)$ to the rest of the moduli space, in particular the Gepner point $1/z = 0$, we utilize the familiar integral representation

$$\tau^{(k)}(z) = \frac{1}{2\pi i}\int \frac{\Gamma\big(\frac{1}{2}-s\big)\Gamma\big(\frac{1}{2}+s\big)\Gamma\big(ks+1\big)}{\prod\Gamma\big(\nu_i s+1\big)} e^{i\pi(s-\frac{1}{2})} z^s\,, \tag{4.6}$$

where the integration contour runs straight up the imaginary axis. For $|z| < R_*$, we close the contour on the positive real axis, pick up the poles at $s = m + \frac{1}{2}$ for $m = 0, 1, \ldots$, and recover (4.3). For $|z| > R^*$, we close on the negative real axis, where we find poles of Γ-functions in the numerator at $s = -m - \frac{1}{2}$ and at $s = -\frac{m}{k}$ for $m = 1, 2, \ldots$. When k is even, the second actually encompass the former. In that case, however, we also have exactly one even weight (ν_5 in our notation) so that there is also a pole in the denominator, and the total pole at $s = -m - \frac{1}{2}$ is first order. To make progress, we separate the terms with half-integer power of z from the terms with powers on the list of exponents of the homogeneous equation,

$$\tau^{(k)}(z) = \tau^{(k)}_1(z) + \tau^{(k)}_2(z)\,, \tag{4.7}$$

where

$$\begin{aligned}
\tau^{(k)}_1(z) &= \sum_{m=0}^{\infty} \frac{\nu_5}{k}(-1)^{\frac{k}{2}+\frac{\nu_5}{2}+1} \frac{\Gamma\big(\nu_5 m + \frac{\nu_5}{2}\big)}{\Gamma\big(km+\frac{k}{2}\big)\prod_{i,\nu_i \text{ odd}}\Gamma\big(1-\nu_i(m+\frac{1}{2})\big)}\, z^{-m-\frac{1}{2}}\,, \\
\tau^{(k)}_2(z) &= -\frac{\pi}{k}\sum_{m=1}^{\infty} \frac{e^{i\pi\left(m-\frac{m}{k}-\frac{1}{2}\right)}}{\cos\pi\frac{m}{k}} \frac{1}{\Gamma(m)\prod\Gamma\big(1-\frac{\nu_i}{k}m\big)}\, z^{-m/k} \ .
\end{aligned} \tag{4.8}$$

In the sum for $\tau^{(k)}_2$, we have to exclude those m for which m/k is a half integer, since we have already attributed these terms to $\tau^{(k)}_1$. On the other hand, all other terms for which $\nu_i m/k$ is integer can be trivially included.

Our next task is to express $\tau^{(k)}_2$ in terms of the solutions of the homogeneous equation. We use the set of solutions of [4],

$$\varpi^{(k)}_j(z) = -\frac{\pi}{k}\sum_{m=1}^{\infty} \frac{e^{i\pi(m-\frac{m}{k})}\, e^{2\pi i j m/k}}{\sin\pi\frac{m}{k}} \frac{1}{\Gamma(m)\prod\Gamma\big(1-\frac{\nu_i}{k}m\big)}\, z^{-m/k}\,, \tag{4.9}$$

for $j = 0, \ldots, k-1$. Comparing (4.8) with (4.9), we find that

$$\tau_2^{(k)}(z) = \sum a_j \varpi_j(z)\,, \tag{4.10}$$

provided the a_j satisfy the equations

$$-i\,\tan\pi\frac{m}{k} = \sum_{j=0}^{k-1} a_j e^{2\pi i j m/k}\,, \tag{4.11}$$

for $m - 0, 1, \ldots, k-1$, and where the l.h.s. is set to 0 for $m = k/2$. Of course, the a_j are not uniquely determined by (4.10), because the $\varpi_j(z)$ satisfy some linear relations owing to the poles in the denominator of (4.9). Following [6, 4], we will use the "period vector at the Gepner point"

$$\varpi^{(k)} = \big(\varpi_2, \varpi_1, \varpi_0, \varpi_{k-1}\big)\,, \tag{4.12}$$

and write

$$\tau_2^{(k)} = \tilde{a}^{(k)} \cdot \varpi^{(k)}\ . \tag{4.13}$$

We have the following results for the vectors $a^{(k)}$ and $\tilde{a}^{(k)}$.

k	$a^{(k)}$	$\tilde{a}^{(k)}$
6	$\frac{1}{3}(0,-2,1,0,-1,2)$	$\frac{1}{3}(2,-2,1,2)$
8	$\frac{1}{4}(0,-3,2,-1,0,1,-2,3)$	$(1,-1,0,1)$
10	$\frac{1}{5}(0,-4,3,-2,1,0,-1,2,-3,4)$	$\frac{1}{5}(2,-4,1,2)$

(4.14)

Also from [4], we extract the analytic continuation matrices between the Gepner basis $\varpi^{(k)}$ and the large volume basis $\Pi^{(k)} = (\Pi_6, \Pi_4, \Pi_2, \Pi_0)$. (This basis is almost the one from (4.2). See [4] for precise definitions.) Namely,

$$\Pi^{(k)} = M^{(k)} \varpi^{(k)}\,, \tag{4.15}$$

with

$$M^{(6)} = \begin{pmatrix} 0 & -1 & 1 & 0 \\ -1 & 0 & 3 & 2 \\ \frac{1}{3} & \frac{1}{3} & -\frac{1}{3} & -\frac{1}{3} \\ 0 & 0 & 1 & 0 \end{pmatrix}\,, \qquad M^{(8)} = \begin{pmatrix} 0 & -1 & 1 & 0 \\ -1 & 0 & 3 & 2 \\ \frac{1}{2} & \frac{1}{2} & -\frac{1}{2} & -\frac{1}{2} \\ 0 & 0 & 1 & 0 \end{pmatrix}\,,$$
$$M^{(10)} = \begin{pmatrix} 0 & -1 & 1 & 0 \\ 0 & 1 & 1 & 1 \\ 1 & 0 & 0 & -1 \\ 0 & 0 & 1 & 0 \end{pmatrix}\,. \tag{4.16}$$

Finally, we record the action of the Gepner monodromy

$$z^{-\frac{1}{k}} \to e^{\frac{2\pi i}{k}} z^{-\frac{1}{k}}\,, \tag{4.17}$$

on the basis $\Pi^{(k)}$ (along the path leading to the above basis transformation). We have $\Pi^{(k)} \to A^{(k)}\Pi^{(k)}$ with

$$A^{(6)} = \begin{pmatrix} -3 & -1 & -6 & 4 \\ -3 & 1 & 3 & 3 \\ 1 & 0 & 1 & -1 \\ -1 & 0 & 0 & 1 \end{pmatrix}, \qquad A^{(8)} = \begin{pmatrix} -3 & -1 & -4 & 4 \\ -2 & 1 & 2 & 2 \\ 1 & 0 & 1 & -1 \\ -1 & 0 & 0 & 1 \end{pmatrix},$$
$$A^{(10)} = \begin{pmatrix} -2 & -1 & -1 & 3 \\ 0 & 1 & 1 & 0 \\ 1 & 0 & 1 & -1 \\ -1 & 0 & 0 & 1 \end{pmatrix}, \tag{4.18}$$

4.2 Monodromy

We now have all expressions at our disposal to discuss the analytic continuation and monodromy properties of the open string periods. After the mirror map, our current ansatz for the B-model version of the domainwall tension with large volume expansion (2.6) is[4]

$$\mathcal{T}_A^{(k)} = \frac{\Pi_2^{(k)}}{2} + \frac{\Pi_0^{(k)}}{4} + d\tau^{(k)}\,, \tag{4.19}$$

where d is a constant. For $k = 8$, the additional domainwall interpolating between the two $\mathbb{RP}^3$ components of $L^{(8)}_{[0,0,0,0,1]}$ has tension

$$\widetilde{\mathcal{T}_A} = \frac{\Pi_4^{(8)}}{2}\,. \tag{4.20}$$

By construction, $\mathcal{T}_A$ and $\widetilde{\mathcal{T}_A}$ have integral large volume monodromy as $t \to t+1$. Namely,

$$t \to t+1: \qquad \begin{array}{l} \mathcal{T}_A \to \Pi_2 - \mathcal{T}_A \\ \widetilde{\mathcal{T}_A} \to \widetilde{\mathcal{T}_A} - \Pi_2 - 2\Pi_0\,. \end{array} \tag{4.21}$$

Consider now the Gepner monodromy, using (4.16) and (4.18). From the splitting (4.7), we see that $\tau_1^{(k)}$ changes sign as we circle $1/z = 0$ once. Since the squareroot is the hallmark of the inhomogeneity, we see that $\mathcal{T}_A$ must come back to minus itself, up to a solution of the homogeneous equation. To ensure that this solution is an integral period, we consider the behaviour of $\tau_2^{(k)}$. Combining (4.13) and (4.18), we find

$$\tau_2^{(k)} \to -\tau_2^{(k)} + \Pi_6^{(k)}\,. \tag{4.22}$$

Since for each $k = 6, 8, 10$, the classical part of the domainwall tension transforms as

$$\mathcal{T}_{A,cl} = \frac{\Pi_2}{2} + \frac{\Pi_0}{4} \to \frac{\Pi_6}{4} + \Pi_2 - \mathcal{T}_{A,cl}\,, \tag{4.23}$$

we see that the minimal value of d that guarantees integrality is

$$d = -\frac{1}{4}\,. \tag{4.24}$$

[4]We use A/B subscript to distinguish the large/small volume basis, and leave the mirror map (3.3) implicit.

The Gepner monodromy then acts as

$$z^{-1/k} \to e^{2\pi i/k} z^{-1/k} : \qquad \begin{array}{l} \mathcal{T}_A \to \Pi_2 - \mathcal{T}_A \\ \widetilde{\mathcal{T}_A} \to \widetilde{\mathcal{T}_A} - \Pi_6 + \Pi_2 + \Pi_0 \ . \end{array} \tag{4.25}$$

Integrality in the last line is ensured by the evenness of the appropriate entries in (4.18). A noteworthy consequence is the invariance of $\mathcal{T}_A$ under the conifold monodromy, resulting from combination of (4.21) and (4.25).

4.3 Domainwall spectrum and final matching of vacua

The domainwall tensions (4.19), (4.20) satisfy the same inhomogeneous Picard-Fuchs equation that we had obtained in section 3. Namely, with $\tilde{c}^{(k)}$ from (4.5) and $d = -1/4$ from (4.24), we find

$$\frac{1}{4}\tilde{c}^{(k)} = c^{(k)} \,, \tag{4.26}$$

where $c^{(k)}$ are the non-zero entries in (3.20). And $\widetilde{\mathcal{T}_A}$ satisfies the homogeneous equation by construction.

The fact that $\mathcal{T}_A^{(k)}$ comes back to minus itself (up to an integral period) in (4.25) means that the corresponding brane vacua are exchanged under Gepner monodromy. This is precisely what we had noted at the end of section 2.

Finally, we test for tensionless domainwalls at the Gepner point. Using (4.13), we find that the leading behaviour of $\mathcal{T}_A$ around $1/z \to 0$ is given by

$$\mathcal{T}_A \sim \sqrt{z} + \tilde{b}^{(k)} \cdot \Pi^{(k)} \,, \tag{4.27}$$

where $\tilde{b}^{(k)} = -\frac{1}{4}(M^{(k)})^{-T}\tilde{a}^{(k)} + (0,0,\frac{1}{2},\frac{1}{4})$, explicitly,

k	$\tilde{b}^{(k)}$
6	$\frac{1}{3}(-2,-1,-3,4)$
8	$(-1,-\frac{1}{2},-1,2)$
10	$\frac{1}{5}(-2,-1,2,4)$

(4.28)

Thus, for $k = 6, 10$, the leading behaviour at $1/z = 0$ is always dominated by a non-vanishing closed string period, and we have no tensionless domainwall.[5] This is exactly what we predicted in section 2 under the identification (2.24), and concludes our discussion for those two models.

We continue with $k = 8$. First of all, we see from (4.28) that by combining $\mathcal{T}_A$ with $\widetilde{\mathcal{T}_A}$, we obtain a tensionless domainwall[6] at the Gepner point, which is again precisely as predicted! In section 3, we had denoted this vaninishing domainwall by $\mathcal{T}_B$, so we identify

$$\mathcal{T}_B = \mathcal{T}_A + \widetilde{\mathcal{T}_A} \ . \tag{4.29}$$

[5]This does not exclude the interesting possibility that there are tensionless domainwalls somewhere else in the moduli space.

[6]This, as well as all remaining statements in this subsection, are understood modulo integral periods. Those correspond to changing Ramond-Ramond flux, which is invisible on the brane. We also leave the mirror map implicit.

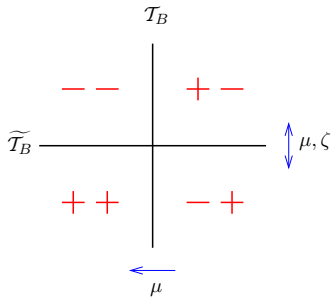

Figure 2: Set of vacua and basis of domainwalls at the Gepner point of $X^{(8)}$.

The other open string period from section 3 satisfies the homogeneous equation, so we have

$$\widetilde{\mathcal{T}_B} = \widetilde{\mathcal{T}_A} \ . \tag{4.30}$$

Now recalling the definitions (2.14) and (3.15) (and ignoring RR-flux, as we said),

$$\mathcal{T}_A = \mathcal{W}_{(\xi,+)} - \mathcal{W}_{(\xi,-)} \,, \qquad \widetilde{\mathcal{T}_A} = \mathcal{W}_{(\xi,\sigma)} - \mathcal{W}_{(-\xi,\sigma)} \,, \tag{4.31}$$

$$\mathcal{T}_B = \mathcal{W}_{\langle +,+\rangle} - \mathcal{W}_{\langle -,+\rangle} \,, \qquad \widetilde{\mathcal{T}_B} = \mathcal{W}_{\langle \mu,\zeta\rangle} - \mathcal{W}_{\langle -\mu,-\zeta\rangle} \,, \tag{4.32}$$

we obtain an exact match of domainwall spectrum if we identify the large volume brane vacua (ξ, σ) with those at the Gepner point $\langle \mu, \zeta \rangle$ according to

$$\mu = \xi \,, \ \zeta = \xi\sigma \ . \tag{4.33}$$

More pictorially, one may compare figure 1 one page 6 with figure 2. The former shows the collection of vacua and interpolating domainwalls at the large volume point in the A-model, while the second illustrates the domainwall spectrum obtained in the B-model at the Gepner point.

5. Discussion and conclusions

In this paper, we have accumulated evidence for a mirror symmetry identification between A-branes defined as the real slices of one-parameter hypersurfaces in weighted projective space and B-branes defined via certain matrix factorizations of the Landau-Ginzburg superpotential. We have made this identification at the level of the holomorphic data, namely the structure of $\mathcal{N} = 1$ supersymmetric vacua on the D-brane worldvolume and the tension of BPS domainwalls between them.

The basic structure is similar to the real quintic studied in [1, 2]. All models have in common that they possess real Lagrangians with $H_1(L, \mathbb{Z}) = \mathbb{Z}_2$. This discrete datum corresponds to a choice of discrete Wilson line. Using mirror symmetry, or just based on considerations of monodromy, one can show that the domainwall tension separating those vacua is captured by an inhomogeneous Picard-Fuchs equation with inhomogeneous term $\sim z^{1/2}$. It is tempting to speculate that this specific type of inhomogeneous extension

will generally describe the domainwall separating the two possible vacua of a D-brane on Lagrangians with $H_1(L,\mathbb{Z}) = \mathbb{Z}_2$.

On a technical level, the key quantity to compute is the exact constant of proportionality of the inhomogeneous term in the Picard-Fuchs equation. We have determined these constants via two orthogonal approaches, namely consistency of monodromies and explicit computations of Abel-Jacobi type, resulting from the B-model matrix factorizations.

The $k = 8$ hypersurface differs slightly from the other models by the fact that the real Lagrangian of interest possesses two disconnected, but homologically equivalent components, and $H_1(L,\mathbb{Z}) = \mathbb{Z}_2 \times \mathbb{Z}_2$. Hence, this geometry has in addition a second discrete open string modulus corresponding to the component the D-brane is wrapped on, as well as a second domainwall, which is formed by a D-brane on the 4-chain separating the two components. The tension of this domainwall is simply a fractional (quantum corrected) closed string period. While this picture is suitable at the large volume point, we made the observation that continuation to the Gepner point induces a "mixing" of these (from a large volume point of view) different moduli. This is another manifestation of the break down of classical geometric concepts in the quantum regime, and perhaps the most interesting lesson of our computations. We conclude with some further consequences.

5.1 Disk instanton numbers

To extract the Ooguri-Vafa invariants [12] from the Gromov-Witten expansion of the domainwall tension, (2.6), we recall that the familiar $1/l^3$-multicover formula is replaced in the open string context by $1/l^2$. In terms of the quantum part of the domainwall tension (4.3), the expansion takes the form

$$\frac{\pi^2}{4}\,\frac{\tau(z(q))}{\varpi_0(z(q))} = \sum_{l,d\ \mathrm{odd}} \frac{n_d^{(0,\mathrm{real})}}{l^2} q^{dl/2}\ . \tag{5.1}$$

The resulting integers $n_d^{(0,\mathrm{real})}$ (see table 3 for some examples) are BPS-invariants in the string/M-theory setup of [12]. Mathematically, they are predicted to be enumerative invariants counting real rational curves in $X^{(k)}$.

It is interesting to note that Ooguri-Vafa integrality also holds for the second domainwall that appears for $X^{(8)}$, see (2.15). Since $\widetilde{\mathcal{T}}_A = \Pi_4/2$, where $\Pi_4 \sim \partial\mathcal{F}$, this integrality can be deduced from the integrality of ordinary closed string instanton numbers (obtained from prepotential $\mathcal{F}$ with $1/l^3$ multi-cover formula). Note however that this is not a totally trivial check because of the relative factors of 2 between open and closed string expansion.

In the absence of direct A-model computations of Gromov-Witten or Ooguri-Vafa invariants, further checks on the enumerative predictions of table 3 can be derived from the computation of loop amplitudes in the topological string.

5.2 One-loop test

As explained in [13, 14], the domainwall tensions that we obtained as solutions of the inhomogeneous Picard-Fuchs equation in the previous sections constitute tree-level data for the computation of topological string amplitudes on the appropriate Calabi-Yau orientifold

n_d	disk instanton numbers for $L^{(6)}_{[M]}$
1	24
3	5880
5	14328480
7	48938353176
9	204639347338560
11	965022386745454392

n_d	disk instanton numbers for $L^{(8)}_{[0,0,0,0,1]}$
1	48
3	65616
5	919252560
7	17535541876944
9	410874634758297216
11	10854343378339853472336

n_d	disk instanton numbers for $L^{(10)}_{[M]}$
1	128
3	2886528
5	465626856320
7	112339926393132928
9	33254907472965538667520
11	11110159357336987759939410816

Table 3: Low degree BPS invariants $n_d^{(0,\text{real})}$ for the three models $X^{(6)}$, $X^{(8)}$, and $X^{(10)}$.

models. Technically, we have an extension of ordinary special geometry to the open string sector, characterized infinitesimally by the two-point function on the disk, Δ. This is related to the tree-level domainwall $\mathcal{T}$ as $\Delta \sim D^2\mathcal{T} - CD\overline{\mathcal{T}}$, where C is the closed string Yukawa coupling (i.e., the infinitesimal invariant of the closed topological string), and D is the covariant derivative on moduli space. Under certain additional conditions (no contribution from open string moduli, tadpole cancellation, further discussed in [27]), the amplitudes for higher worldsheet topology are then recursively constrained by the extended holomorphic anomaly equation of [13], which is a generalization of the BCOV equations [16]. The main obstacle to carrying out this program is the holomorphic ambiguity, which at present is not very well understood in the open/unoriented sector.

For the one-loop amplitudes however, we have a complete proposal [14], generalizing the result of [15]. We can therefore just plug in the tree-level data into this formula, and extract [12, 28, 14] one-loop BPS invariants for our three one-parameter hypersurfaces. One of the checks alluded to above is the following equality of tree-level and one-loop enumerative invariants on $X^{(6)}$:

$$k = 6: \qquad n_1^{(0,\text{real})} = n_2^{(1,\text{real})} = 24\ . \tag{5.2}$$

We view this as the real version of the coincidence of the complex enumerative invariants (see, e.g., [29])

$$k = 6: \qquad n_1^{(0)} = n_2^{(1)} = 7884\,, \tag{5.3}$$

which arises from the relation between the corresponding intersection problems. The equality (5.2) gives evidence that this relation persists in the real version of the problem. Another check is the necessary equality of complex and real enumerative invariants modulo 2, i.e.,

$$k = 6, 8, 10: \qquad n_d^{(\hat{g},\text{real})} = n_d^{(\hat{g})} \bmod 2\,, \tag{5.4}$$

holds for all three models, all d, and $\hat{g} = 0, 1$.

Another interesting aspect of the loop computations derives from the disconnectedness of the real slice of $X^{(8)}$. As observed in [14], it appears that in order to obtain a satisfactory BPS interpretation for open topological string amplitudes on compact Calabi-Yau manifold, one has to consider an orientifold model and choose a D-brane configuration that cancels the tadpoles. In our models, we naturally choose the orientifold action that we used to define the D-branes, and put exactly one D-brane on top of the orientifold plane. For $k = 8$, however, the orientifold plane is disconnected, and there are more tadpole cancelling D-brane configurations (ten, using just the branes we discussed). In other words, the topological string amplitudes are a function of four discrete moduli $(\xi_1, \sigma_1, \xi_2, \sigma_2)$, in addition to the closed string modulus t. We have computed this function at one-loop and found an integral BPS expansion in all sectors. We will return to this elsewhere.

5.3 Outlook

The integrality of the $n_d^{(0,\text{real})}$ from table 3 is a strong check that our overall picture is consistent. Note however that the overall normalization of these numbers is not fixed by integrality alone (in particular, all $n_d^{(0,\text{real})}$ are divisible by the first number, $n_1^{(0,\text{real})}$). Our confidence in the enumerative predictions therefore mainly rests on the agreement between the two different computations of this normalization constant, monodromy and Abel-Jacobi. As further comfort, we note that the corresponding predictions on the quintic [1] have been verified in [30] using the open Gromov-Witten theory of [31] and localization on the space of maps to the ambient $\mathbb{P}^4$. It would be interesting to verify our predictions in the weighted case by this or other methods.

One might also ask if similar considerations could be applied as well to Lagrangians with more general torsion $H_1(L, \mathbb{Z}) = \mathbb{Z}_p$. A natural guess would be that the domainwalls separating these vacua are similarly captured on the B-side via an inhomogeneous extension of the ordinary Picard-Fuchs equations of the form $\sim z^{1/p}$. It would be interesting to find some explicit examples which support this proposal.

Acknowledgments

We would like to thank Manfred Herbst and Wolfgang Lerche for valuable discussions. The work of D.K. is supported by an EU Marie-Curie EST fellowship. The work of J.W. was supported in part by the Swiss National Science Foundation, and by the NSF under grant number PHY-0503584.

A. Inhomogeneous Picard-Fuchs equation via Griffiths-Dwork

In the following, we will give some more details of the main computation of section (3.2), i.e. the evaluation of (3.16). In order to be able to evaluate (3.16), we first need to derive the exact parts $\tilde{\beta}^{(k)}$ of the inhomogeneous Picard-Fuchs equations covering the (extended) periods of $Y^{(k)}$. We will achieve this via the Griffiths-Dwork method (see for instance [3]):

The fundamental weighted homogeneous differential form of the ambient space is given by

$$\omega^{(k)} = \sum_{i=1}^{5} (-1)^{i-1} \nu_i x_i dx_1 \wedge \ldots \wedge \widehat{dx_i} \wedge \ldots \wedge dx_5 \,, \tag{A.1}$$

where ν_i are the weights and x_i the homogenous coordinates of the ambient weighted $\mathbb{P}^4$. For later convenience, we define $\omega_i^{(k)} := \partial_i \omega^{(k)}$.

The holomorphic 3-form is given by

$$\Omega = Res_{W^{(k)}=0} \tilde{\Omega} \,, \tag{A.2}$$

with $\tilde{\Omega} = \frac{\omega^{(k)}}{W^{(k)}}$. For simplicity, the $^{(k)}$ indices are implicitly understood in the following. Then, the fundamental period

$$w_0 = \int_\Gamma \Omega \,, \tag{A.3}$$

where Γ is usually a 3-cycle, here however we allow Γ to have a boundary $\partial\Gamma$, evaluates to

$$w_0 = \int_\Gamma Res_{W=0} \tilde{\Omega} = \int_{T_\epsilon(\Gamma)} \tilde{\Omega} \,, \tag{A.4}$$

where T_ϵ is a small tube around Γ. From that we obtain

$$\partial_\psi^l w_0 = l! \int_{T_\epsilon(\Gamma)} \frac{(x_1 x_2 x_3 x_4 x_5)^l}{W^{l+1}} \omega \,, \tag{A.5}$$

where we have implicitly assumed that there will be no contribution of derivatives acting on the chain. That this is indeed the case will be explicitly verified for the models under consideration.

For $l = 4$ we can express $\partial_\psi^l w_0$ in terms of lower derivatives using the equations of motion $\partial_i W = 0$ and "partial integration" (Griffith's reduction of pole order) and obtain in this way a differential equation of (inhomogeneous) Picard-Fuchs type satisfied by w_0. The calculation is lengthy, but straight-forward.

A.1 $Y^{(6)}$

Using the Griffiths-Dwork method as described above and the relation

$$\begin{aligned} \psi^2(1-\psi^6)(x_1^4 x_2^4 x_3^4 x_4^4 x_5^4) = {} & \psi^7(x_1^3 x_2^3 x_3^3 x_4^3 x_5^4)\partial_5 W + \psi^6(x_1^2 x_2^2 x_3^2 x_4^3 x_5^5)\partial_4 W \\ & + \psi^5(x_1 x_2 x_3^2 x_4^7 x_5^4)\partial_3 W + \psi^4(x_2 x_3^6 x_4^6 x_5^3)\partial_2 W \\ & + \psi^3(x_2^5 x_3^5 x_4^5 x_5^2)\partial_1 W + \psi^2(x_1^4 x_2^4 x_3^4 x_4^4 x_5^2)\partial_5 W \,, \end{aligned} \tag{A.6}$$

we obtain the inhomogeneous Picard-Fuchs equation

$$\tilde{\mathcal{L}}^{(6)} = \psi^2(1-\psi^6)\partial_\psi^4 - 2\psi(1+5\psi^6)\partial_\psi^3 + (2-25\psi^6)\partial_\psi^2 - 15\psi^5\partial_\psi - \psi^4 = d\tilde{\beta} \,, \tag{A.7}$$

with exact part

$$\begin{aligned}\tilde{\beta}^{(6)} =&\frac{6}{W^4}\left[\psi^7 x_1^3x_2^3x_3^3x_4^3x_5^4\omega_5+\psi^6 x_1^2x_2^2x_3^2x_4^3x_5^5\omega_4+\psi^5 x_1x_2x_3^2x_4^7x_5^4\omega_3\right.\\&\left.+\psi^4 x_2x_3^6x_4^6x_5^3\omega_2+\psi^3 x_2^5x_3^5x_4^5x_5^2\omega_1+\psi^2 x_1^4x_2^4x_3^4x_4^4x_5^2\omega_5\right]\\&+\frac{2}{W^3}\left[3\psi^6 x_1^2x_2^2x_3^2x_4^2x_5^3\omega_5+2\psi^5 x_1x_2x_3x_4^7x_5^2\omega_5+3\psi^6 x_1^2x_2^2x_3^2x_4^3x_5^2\omega_4\right.\\&\left.+\psi^4 x_3^6x_4^6x_5\omega_5+\psi^5 x_1x_2x_3^2x_4^7x_5\omega_3-2\psi x_1^3x_2^3x_3^3x_4^3x_5\omega_5\right]\\&+\frac{1}{W^2}\left[6\psi^5 x_1x_2x_3x_4^2x_5\omega_4+\psi^4 x_3^6x_4\omega_4+\psi^5 x_1x_2x_3^2x_4x_5\omega_3+x_1^2x_2^2x_3^2x_4^2\omega_5\right]\\&+\frac{1}{W}\left[\psi^4 x_3\omega_3\right]\ .\end{aligned}\tag{A.8}$$

The next step in the evaluation of (3.16) is to define a proper tube $T_\epsilon(\partial\Gamma)$, where we have for $Y^{(6)}$: $\partial\Gamma = C_+^{(6)} - C_-^{(6)}$ with $C_\zeta^{(6)}$ given in (3.7). For simplicity, we set $\alpha^{(6)} = i$ and drop the $^{(6)}$ indices in the following. Observe that the curves C_ζ possess two components distinguished by $\gamma = \pm 1$, i.e. $C_\zeta = C_\zeta^+ + C_\zeta^-$ with

$$C_\zeta^\gamma = \{x_1 = i\zeta x_2, x_3 = ix_4, x_5 = i^{\frac{-\zeta-1}{2}}\gamma\sqrt{3\psi}x_1x_3\}\ .\tag{A.9}$$

Note that the curves intersect in three points:

$$p_1^\zeta := \{x_1 = i\zeta x_2, x_3 = x_4 = x_5 = 0\},\ p_2 := \{x_3 = ix_4, x_1 = x_2 = x_5 = 0\}\ .\tag{A.10}$$

For the same reasons as in the quintic case discussed in [2], only the neighborhood of the set of points $\{p_1^\zeta, p_2^\zeta := p_2\}$ gives a contribution to the integral over the tube $T_\epsilon(\partial\Gamma)$. Hence, the integral (3.16) splits up into

$$\int_{T_\epsilon(\partial\Gamma)}\tilde{\beta} = \sum_{\zeta,\gamma,i}\zeta\int_{T_\epsilon(C_\zeta^\gamma;p_i^\zeta)}\tilde{\beta}\,,\tag{A.11}$$

where we define the tubes $T_\epsilon(C_\zeta^\gamma; p_i^\zeta)$ around C_ζ^γ near p_i^ζ momentarily:

The region around the points p_i^ζ is best described in the following two local charts of the ambient weighted $\mathbb{P}^4$:

$$U_1:\ x_i \to \frac{x_j}{x_1^{\nu_j}}\,,\ U_2:\ x_j \to \frac{x_j}{x_3^{\nu_j}}\,,\tag{A.12}$$

where $p_i^\zeta \subset U_i$.

Let us start with the region around p_1^ζ: Changing to the inhomogeneous coordinates of $(A.12)$, i.e.

$$T' := \frac{x_2}{x_1}\,,\ X' := \frac{x_3}{x_1}\,,\ Y' := \frac{x_4}{x_1}\,,\ Z' := \frac{x_5}{x_1^2}\,,\tag{A.13}$$

and performing subsequently the coordinate change

$$T' \to i\zeta T\,,\ Y' \to -iY\,,\ X' \to X+Y+Z\,,\ Z' \to i^{\frac{-\zeta-1}{2}}\gamma(1+\sqrt{3\psi}(Y+Z))\,,\tag{A.14}$$

we obtain a more convenient parameterization of C^γ_ζ and p^ζ_1:

$$\begin{aligned} C^\gamma_\zeta &= \left\{ T = -1, X = -Z = \frac{1}{\sqrt{3\psi}} \right\}, \\ p^\zeta_1 &= \left\{ T = -1, X = -Z = \frac{1}{\sqrt{3\psi}}, Y = 0 \right\} . \end{aligned} \tag{A.15}$$

Observe that the curves C^γ_ζ are parametrized in their respective coordinate systems by the single coordinate $Y = re^{i\phi}$, and intersects with the other curves at $r = 0$.

We now define tubes $T^{\zeta\gamma}_\epsilon$ around the curves C^γ_ζ by requiring that $T^{\zeta\gamma}_\epsilon$ lies outside of $Y^{(6)}$ inside a small neighborhood of p^ζ_1 ($0 \leq r < r^*$) and inside of $P^{(6)}$ else ($r \geq r^*$). Therefore, consider the normal vectors

$$v_{\zeta\gamma} = a_{\zeta\gamma} D_T - \gamma \frac{i^{\frac{-\zeta-1}{2}}}{2} e^{-2i\phi} \partial_X + \gamma \frac{i^{\frac{-\zeta-1}{2}}}{2} e^{-2i\phi} \partial_Z \,, \tag{A.16}$$

with

$$a := \frac{f(r)}{1 + \gamma i^{\frac{\zeta+1}{2}} \sqrt{3\psi^3} Y^3} \,, \tag{A.17}$$

where $f(r)$ is a non-negative C^∞ function with $f(0) = 1$ and $f(r) = 0$ for $r \geq r^* > 0$. Clearly $v_{\zeta\gamma}$ point inside of $P^{(6)}$ for $r > r^*$. Note that the definition of $a_{\zeta\gamma}$ naturally fixes the point r^*. To see that, note if we define $r^* = (3\psi^3)^{-1/6}$, $f(r^*)$ must vanish, since otherwise $a_{\zeta\gamma}$ would have poles at r^*. For reasons that will become clear later, we require as well that the first derivative $f'(r)$ vanishes at $r \geq r^* > 0$.

One easily checks that

$$D_{v_{\zeta\gamma}} W|_{C^\gamma_\zeta} = f(r) + \sqrt{3\psi^3} r^2 > 0 \,, \tag{A.18}$$

hence $v_{\zeta\gamma}$ points outside of $Y^{(6)}$ and thus we can use $v_{\zeta\gamma}$ to define proper tubes $T^{\zeta\gamma}_\epsilon$. In detail, the tubes are parameterized in local coordinates by

$$T = -1 + \tilde{\epsilon} a \,, \; X = -Z = \frac{1}{\sqrt{3\psi}} - \gamma \frac{i^{\frac{-\zeta-1}{2}}}{2} \tilde{\epsilon} e^{-2i\phi} \,, \tag{A.19}$$

where $\tilde{\epsilon} = e^{i\chi}\epsilon$ and $\chi \in [0, 2\pi]$.

For the evaluation of (A.11) we need to express $\tilde{\beta}$ in the coordinates (A.14), restrict to the respective tubes and perform the integration over

$$\int_0^\infty dr \int_0^{2\pi} d\phi \int_0^{2\pi} d\chi \,. \tag{A.20}$$

Since the terms occurring in $\tilde{\beta}$ are proportional to $\frac{\omega_i}{W^l}$, we especially need $\omega_i|_{T^{\zeta\gamma}_\epsilon}$. After going to the chart U_1 and restricting to $X' = iY'$, we infer from (A.1) that $\omega_i = 0$ for $i \notin \{3, 4\}$ and

$$\omega_4 = -i\omega_3 = dT' \wedge dX' \wedge dZ' \,. \tag{A.21}$$

Changing to the coordinates (A.14) then yields

$$dT' \wedge dX' \wedge dY' = i^{\frac{-\zeta+1}{2}} \zeta\gamma \sqrt{3\psi} dT \wedge dX \wedge dY \,, \tag{A.22}$$

which restricts on the tubes $T_\epsilon^{\zeta\gamma}$ to

$$dT \wedge dX \wedge dY|_{T_\epsilon^{\zeta\gamma}} = -i^{\frac{-\zeta-1}{2}} \gamma e^{-i\phi} a \left(1 - \frac{r f'(r)}{2f(r)}\right) \tilde{\epsilon}^2 dr \wedge d\phi \wedge d\chi \,. \tag{A.23}$$

We have now everything at our disposal to infer the contribution of the integrals over the tubes $T_\epsilon(C_\zeta^\gamma; p_1^\zeta)$ to (A.11). For performing the explicit calculation, note that only terms which do not come in powers of $\tilde{\epsilon}$ can survive the integration over $d\chi$. Hence, the integration over $d\chi$ simply yields a factor of 2π. For the integration over $d\phi$ it is more convenient to perform the variable transformation $e^{i\phi} \to z$, with $z \in \mathbb{C}$. In this coordinate, the integral becomes a line integral around the unit circle in the complex plane and only terms can contribute that have poles in the unit disk. Combined with the property $f(r) = f'(r) = 0$ for $r \geq r^*$, it is easy to see that only terms can contribute which do not come in powers of z in the nominator.

Performing the explicit calculation we infer that there is no contribution from the integrals over the tubes $T_\epsilon(C_\zeta^\gamma; p_1^\zeta)$ to (A.11).

It remains to evaluate the contribution of $T_\epsilon(C_\zeta^\gamma; p_2)$ to (A.11): For that, we need to perform the same calculations as above in the coordinate chart U_2 which includes p_2. Hence, we take the inhomogeneous coordinates

$$T' := \frac{x_4}{x_3} \,,\; X' := \frac{x_1}{x_3} \,,\; Y' := \frac{x_2}{x_3} \,,\; Z' := \frac{x_5}{x_3^2} \,, \tag{A.24}$$

and perform the same coordinate redefinitions as in (A.14) in order to obtain (A.15). However, this time p_1^ζ corresponds to p_2. Due to the symmetry of W, the tubes $T_\epsilon^{\zeta\gamma}$ have the same parameterization and we can still use (A.16)–(A.23), if we replace

$$\omega_4 \to \omega_2 \,,\; \omega_3 \to \omega_1 \,. \tag{A.25}$$

Performing the explicit calculation similar as in chart U_1, we infer that we obtain contributions from the term

$$\int_{T_\epsilon(C_\zeta^\gamma; p_2)} \frac{6\psi^4 x_2 x_3^6 x_4^6 x_5^3 \omega_2}{W^4} = \zeta \frac{2}{3} \pi^2 . \tag{A.26}$$

Note that we have taken an additional normalization factor of 6^{-1} due to G_{fix} given in table 1 into account (p_2 is a singular point).

It remains to show that the underlying assumption that we have no contribution from derivatives acting on $T_\epsilon(\Gamma)$ indeed holds. The argumentation is as in [2]. For that, note that the normal vectors implementing first order deformations of C_ζ^γ are given by

$$n_{\zeta\gamma} = -i^{\frac{\zeta+1}{2}} \gamma \frac{x_5}{\sqrt{3\psi}} \frac{1}{2\psi} (\partial_3 - i\partial_4) \,. \tag{A.27}$$

Hence, we have that

$$n_{\zeta\gamma}\omega = -i^{\frac{\zeta+1}{2}} \gamma \frac{x_5}{\sqrt{3\psi}} \frac{1}{2\psi} (\omega_3 - i\omega_4) = 0 \,, \tag{A.28}$$

where we used (A.21).

A.2 $Y^{(8)}$

The discussion of the remaining two models $Y^{(8)}$ and $Y^{(10)}$ is very similar to $Y^{(6)}$, hence we will be brief:

For $Y^{(8)}$ we use the relation

$$\begin{aligned}\psi^3(1-\psi^8)(x_1^4x_2^4x_3^4x_4^4x_5^4) =& \psi^{10}(x_1^3x_2^3x_3^3x_4^3x_5^4)\partial_5 W + \psi^9(x_1^2x_2^2x_3^2x_4^3x_5^4)\partial_4 W\\ &+ \psi^8(x_1x_2x_3^2x_4^9x_5^3)\partial_3 W + \psi^7(x_2x_3^8x_4^8x_5^2)\partial_2 W\\ &+ \psi^6(x_2^7x_3^7x_4^7x_5)\partial_1 W + \psi^5(x_1^6x_2^6x_3^6x_4^6x_5)\partial_5 W\\ &+ \psi^4(x_1^5x_2^5x_3^5x_4^5x_5^2)\partial_5 W + \psi^3(x_1^4x_2^4x_3^4x_4^4x_5^3)\partial_5 W\,,\end{aligned} \tag{A.29}$$

to obtain the inhomogeneous Picard-Fuchs equation

$$\tilde{\mathcal{L}}^{(8)} = \psi^3(1-\psi^8)\partial_\psi^4 - \psi^2(6+10\psi^8)\partial_\psi^3 + 5\psi(3-5\psi^8)\partial_\psi^2 - 15(1+\psi^8)\partial_\psi - \psi^7 = d\tilde{\beta}\,, \tag{A.30}$$

with exact part

$$\begin{aligned}\tilde{\beta}^{(8)} =& \frac{6}{W^4}\left[\psi^{10}x_1^3x_2^3x_3^3x_4^3x_5^4\omega_5 + \psi^9x_1^2x_2^2x_3^2x_4^3x_5^4\omega_4 + \psi^8x_1x_2x_3^2x_4^9x_5^3\omega_3 + \psi^7x_2x_3^8x_4^8x_5^2\omega_2\right.\\ &\left. + \psi^6x_2^7x_3^7x_4^7x_5\omega_1 + \psi^5x_1^6x_2^6x_3^6x_4^6x_5\omega_5 + \psi^4x_1^5x_2^5x_3^5x_4^5x_5^2\omega_5 + \psi^3x_1^4x_2^4x_3^4x_4^4x_5^3\omega_5\right]\\ &+ \frac{2}{W^3}\left[3\psi^9x_1^2x_2^2x_3^2x_4^2x_5^3\omega_5 + 2\psi^8x_1x_2x_3x_4^9x_5^2\omega_5 + 2\psi^9x_1^2x_2^2x_3^2x_4^{10}x_5\omega_5\right.\\ &+2\psi^{10}x_1^3x_2^3x_3^3x_4^4x_5\omega_4 - 2\psi^{10}x_1^3x_2^3x_3^3x_4^3x_5^2\omega_5 + \psi^7x_3^8x_4^8x_5\omega_5 + \psi^8x_1x_2x_3^9x_4^2x_5\omega_4\\ &\left.+\psi^9x_1^2x_2^2x_3^3x_4^2x_5^2\omega_3 - 6\psi^2x_1^3x_2^3x_3^3x_4^3x_5^2\omega_5 - 3\psi^3x_1^4x_2^4x_3^4x_4^4x_5\omega_5 - \psi^4x_1^5x_2^5x_3^5x_4^5\omega_5\right]\\ &+ \frac{1}{W^2}\left[4\psi^8x_1x_2x_3x_4^2x_5\omega_4 + 2\psi^9x_1^2x_2^2x_3^2x_4^3\omega_4 - 6\psi^9x_1^2x_2^2x_3^2x_4^2x_5\omega_5 + \psi^7x_3^8x_4\omega_4\right.\\ &\left. + 3\psi^8x_1x_2x_3^2x_4x_5\omega_3 + 15\psi x_1^2x_2^2x_3^2x_4^2x_5\omega_5 + 3\psi^2x_1^3x_2^3x_3^3x_4^3\omega_5\right]\\ &+ \frac{1}{W}\left[\psi^7x_3\omega_3 - 15x_1x_2x_3x_4\omega_5\right]\,.\end{aligned} \tag{A.31}$$

In order to evaluate (3.16), we need to define proper tubes around the curves $C^{(8)}_{\langle\mu,\zeta\rangle}$. For simplicity, in the following we will just discuss the $C^{(8)}_{\langle-,\zeta\rangle}$ part. The $C^{(8)}_{\langle+,\zeta\rangle}$ part can be discussed similarly and the results just differ by an overall sign[7] (therefore the μ in (3.17)). Hence, let us consider the curves

$$C_{\langle-,\zeta\rangle} := \{x_1 = \alpha^\zeta x_2, x_3 = \alpha x_4, x_5 = 2\alpha^{-\zeta-1}\psi x_1^2x_3^2\}\,. \tag{A.32}$$

In the following we will denote these curves simply as C_ζ and we will implicitly set $\alpha = e^{i\pi/8}$. The two curves intersect in the point

$$p := \{x_3 = \alpha x_4, x_1 = x_2 = x_5 = 0\}\,. \tag{A.33}$$

[7] In fact, this must be so since by general principles, the total intersection of the hypersurface with a plane should give a vanishing result.

As a consequence, (A.11) reduces for $Y^{(8)}$ to

$$\int_{T_\epsilon(\partial\Gamma)} \tilde{\beta} = \sum_\zeta \zeta \int_{T_\epsilon(C_\zeta;p)} \tilde{\beta} \ . \tag{A.34}$$

For the evaluation of (A.34), we go to the local chart U_2 defined in (A.24) and perform the variable redefinitions

$$T' \to -\alpha^{-1}T \, , \ Y' \to \alpha^{-\zeta}Y \, , \ X' \to X+Y+Z \, , \ Z' \to \alpha^{-\zeta-1}(1+\sqrt{2\psi}(Y+Z))^2 \ . \tag{A.35}$$

Then, we have

$$\begin{aligned} C_\zeta &= \left\{ T=-1, X=-Z=\frac{1}{\sqrt{2\psi}} \right\} , \\ p &= \left\{ T=-1, X=-Z=\frac{1}{\sqrt{2\psi}}, Y=0 \right\} . \end{aligned} \tag{A.36}$$

The tubes T_ϵ^ζ around C_ζ are parameterized similar as for $Y^{(6)}$ via normal vectors v_ζ defined by

$$v_\zeta = a_\zeta \partial_T - \frac{i}{4}\alpha^{2(\zeta-1)}e^{-3i\phi}\partial_X + \frac{i}{4}\alpha^{2(\zeta-1)}e^{-3i\phi}\partial_Z \, , \tag{A.37}$$

with

$$a_\zeta := \frac{f(r)}{1-2i\zeta\alpha^{2(\zeta-1)}\psi^2 Y^4} \ . \tag{A.38}$$

This choice ensures that

$$D_{v_\zeta} W|_{C_\zeta} = f(r) + \psi^3 r^3 > 0 \, , \tag{A.39}$$

such that T_ϵ^ζ is well defined.

Thus, the tubes T_ϵ^ζ are locally parameterized by

$$T = -1 + \tilde{\epsilon}a \, , \ X = -Z = \frac{1}{\sqrt{2\psi}} - \tilde{\epsilon}\frac{i}{4}\alpha^{2(\zeta-1)}e^{-3i\phi} \, , \tag{A.40}$$

where $\tilde{\epsilon} = e^{i\chi}\epsilon$.

As a last piece, we need the restriction of the forms ω_i to T_ϵ^ζ: Going to the chart U_2 and restricting to $X' = \alpha^\zeta Y'$, we directly infer that $\omega_i = 0$ for $i \notin \{1,2\}$ and that

$$\omega_2 = -\alpha^\zeta \omega_1 = dT' \wedge dX' \wedge dZ' \ . \tag{A.41}$$

Changing to the coordinates (A.35) then yields

$$dT' \wedge dX' \wedge dZ' = -2\alpha^{-2-\zeta}\sqrt{2\psi}(1+\sqrt{2\psi}(Y+Z))dT \wedge dX \wedge dY \ . \tag{A.42}$$

Further,

$$dT \wedge dX \wedge dY|_{T_\epsilon^\zeta} = -i\frac{3}{4}\alpha^{2(\zeta-1)}ae^{-2i\phi}\tilde{\epsilon}^2 \left(1 - \frac{rf'(r)}{3f(r)}\right) dr \wedge d\phi \wedge d\chi \ . \tag{A.43}$$

Thus,

$$\begin{aligned}\omega_2|_{T^\zeta_\epsilon} &= -\alpha^\zeta \omega_1|_{T^\zeta_\epsilon} \\ &= i3\alpha^{-4+\zeta} a\psi e^{-2i\phi}\left(re^{i\phi}+\frac{i}{4}\alpha^{2(\zeta-1)}e^{-3i\phi}\tilde{\epsilon}\right)\tilde{\epsilon}^2\left(1-\frac{rf'(r)}{3f(r)}\right)dr\wedge d\phi\wedge d\chi\ .\end{aligned} \tag{A.44}$$

We have now everything at our disposal to calculate (A.34). After performing the calculations, we infer that we have a contribution from the term

$$\int_{T_\epsilon(C_\zeta;p)}\frac{6\psi^6 x_2^7 x_3^7 x_4^7 x_5\omega_1}{W^4} = \zeta 3\pi^2\psi^2\,, \tag{A.45}$$

where we included an additional normalization factor of 4^{-1}, similar as in the $Y^{(6)}$ case.

Similar as for X(6), we infer from the normal vector

$$n_\zeta = -\frac{\alpha^{\zeta+1}}{4\psi^2}\frac{x_5}{x_1}(\partial_1+\alpha^{-\zeta}\partial_2)\ . \tag{A.46}$$

that

$$n_\zeta\omega = -\frac{\alpha^{\zeta+1}}{4\psi^2}\frac{x_5}{x_1}(\omega_1+\alpha^{-\zeta}\omega_2) = 0\,, \tag{A.47}$$

where we used (A.41). Hence, the underlying assumption that we have no contribution from derivatives acting on $T_\epsilon(\Gamma)$ holds.

A.3 $Y^{(10)}$

For $Y^{(10)}$ we use the relation

$$\begin{aligned}\psi^3(1-\psi^{10})(x_1^4x_2^4x_3^4x_4^4x_5^4) =& \psi^{12}(x_1^3x_2^3x_3^3x_4^3x_5^4)\partial_5 W+\psi^{11}(x_1^2x_2^2x_3^2x_4^3x_5^4)\partial_4 W\\ &+\psi^{10}(x_1x_2x_3^2x_4^6x_5^3)\partial_3 W+\psi^9(x_2x_3^{10}x_4^5x_5^2)\partial_2 W\\ &+\psi^8(x_2^9x_3^9x_4^4x_5)\partial_1 W+\psi^7(x_1^8x_2^8x_3^8x_4^3x_5)\partial_5 W\\ &+\psi^6(x_1^7x_2^7x_3^7x_4^2x_5^2)\partial_5 W+\psi^5(x_1^6x_2^6x_3^6x_4x_5^3)\partial_5 W\\ &+\psi^4(x_1^5x_2^5x_3^5x_5^4)\partial_5 W+\psi^3(x_1^4x_2^4x_3^4x_5^4)\partial_4 W\,,\end{aligned} \tag{A.48}$$

to obtain the inhomogeneous Picard-Fuchs equation

$$\tilde{\mathcal{L}}^{(10)} = \psi^3(1-\psi^{10})\partial_\psi^4-10\psi^2(1+\psi^{10})\partial_\psi^3+5\psi(7-5\psi^{10})\partial_\psi^2-5(7+3\psi^{10})\partial_\psi-\psi^9 = d\tilde{\beta}\,, \tag{A.49}$$

with exact part

$$\begin{aligned}\tilde{\beta}^{(10)} =&\frac{6}{W^4}\left[\psi^{12}x_1^3x_2^3x_3^3x_4^3x_5^4\omega_5+\psi^{11}x_1^2x_2^2x_3^2x_4^3x_5^4\omega_4+\psi^{10}x_1x_2x_3^2x_4^6x_5^3\omega_3\right.\\&+\psi^9x_2x_3^{10}x_4^5x_5^2\omega_2+\psi^8x_2^9x_3^9x_4^4x_5\omega_1+\psi^7x_1^8x_2^8x_3^8x_4^3x_5\omega_5+\psi^6x_1^7x_2^7x_3^7x_4^2x_5^2\omega_5\\&\left.+\psi^5x_1^6x_2^6x_3^6x_4x_5^3\omega_5+\psi^4x_1^5x_2^5x_3^5x_5^4\omega_5+\psi^3x_1^4x_2^4x_3^4x_5^4\omega_4\right]\\&+\frac{2}{W^3}\left[3\psi^{11}x_1^2x_2^2x_3^2x_4^2x_5^3\omega_5+2\psi^{10}x_1x_2x_3x_4^6x_5^2\omega_5+2\psi^{11}x_1^2x_2^2x_3^2x_4^3x_5^2\omega_4\right.\\&+\psi^9x_3^{10}x_4^5x_5\omega_5+\psi^{10}x_1x_2x_3^{11}x_4^2x_5\omega_4+\psi^{11}x_1^2x_2^2x_3^3x_4^2x_5^2\omega_3+7\psi^5x_1^6x_2^6x_3^6x_4x_5\omega_5\\&-10\psi^2x_1^3x_2^3x_3^3x_4^3x_5^2\omega_5-10\psi^3x_1^4x_2^4x_3^4x_4^4x_5\omega_5-10\psi^4x_1^5x_2^5x_3^5x_4^5\omega_5\\&\left.-10\psi^5x_1^6x_2^6x_3^6x_4^2\omega_4-\psi^6x_1^7x_2^7x_3^7x_4^2\omega_5\right]\\&+\frac{1}{W^2}\left[5\psi^{10}x_1x_2x_3x_4^2x_5\omega_4+2\psi^{10}x_1x_2x_3^2x_4x_5\omega_3+35\psi x_1^2x_2^2x_3^2x_4^2x_5\omega_5+\psi^9x_3x_4^5\omega_3\right.\\&\left.+5\psi^2x_1^3x_2^3x_3^3\omega_5+5\psi^3x_1^4x_2^4x_3^4\omega_4+13\psi^4x_1^5x_2^5x_3^5\omega_5+10\psi^2x_1^3x_2^3x_3^3x_4^3\omega_5\right]\\&+\frac{1}{W}\left[\psi^9x_4\omega_4-35x_1x_2x_3x_4\omega_5\right]\ .\end{aligned}\tag{A.50}$$

It is easy to see that the curve for $Y^{(10)}$ given in (3.7) can be obtained by the intersection $P'\cap Y^{(10)}$, with the plane

$$P':=\left\{x_1=\alpha^\zeta x_2,\frac{1}{\sqrt{5}}\alpha^5x_3^5+x_5-\psi x_1x_2x_3x_4=0\right\}.\tag{A.51}$$

By the principle mentioned in the footnote on page 28, we can (up to a sign) use either of the components of $P'\cap Y^{(10)}$, i.e., either (3.7) or the curve $x_4^2=0$. The latter curve is however also contained in the intersection of $Y^{(10)}$ with some different planes, and for incidental reasons, we prefer to present the evaluation of the integral in one of these alternative planes. More explicitly, the curve from (3.7) is equivalent to the curve

$$C_\zeta^\gamma:=\left\{x_1=i\zeta x_2,x_5=i\frac{1}{5^{1/2}}x_3^5,x_4^2=\gamma\sqrt{\zeta}\sqrt{5^{1/2}\psi x_1x_3^3}\right\}\ .\tag{A.52}$$

with $\gamma=\pm1$, which we obtain from $P\cap Y^{(10)}$, where P is related to P' via the coordinate transformation $x_5\to x_5+\psi x_1x_2x_3x_4$. Similar as the curve for $Y^{(6)}$, the C_ζ curve splits into two components, i.e. $C_\zeta=C_\zeta^+ + C_\zeta^-$.

The component curves meet in three points:

$$p_1^\zeta=\{x_1=i\zeta x_2,x_3=x_4=x_5=0\},\ p_2=\left\{x_5=i\frac{1}{5^{1/2}}x_3^5,x_1=x_2=x_4=0\right\}\ .\tag{A.53}$$

In order to evaluate (A.11), we go to the local chart U_1 given by (A.13) and perform the following variable redefinitions:

$$\begin{aligned}T'\to i\zeta T\,,\ Y'\to i5^{-1/2}Y^{10}\,,\ X'\to(X+Y+Z)^2\,,\\ Z'\to\gamma^{1/2}\zeta^{1/4}(1+5^{1/24}\psi^{1/12}(Y+Z))^3\ .\end{aligned}\tag{A.54}$$

Then,

$$C_\zeta^\gamma = \left\{ T = -1, X = -Z = \frac{1}{\sqrt{5^{1/12}\psi^{1/6}}} \right\},$$
$$p_1^\zeta = \left\{ T = -1, X = -Z = \frac{1}{\sqrt{5^{1/12}\psi^{1/6}}}, Y = 0 \right\}. \tag{A.55}$$

We define the tubes $T_\epsilon^{\zeta\gamma}$ via the normal vectors

$$v_{\zeta\gamma} = a_{\zeta\gamma}\partial_T - \frac{\gamma^{3/2}\zeta^{5/4}}{12\cdot 5^{-3/8}} e^{-14i\phi}\partial_X + \frac{\gamma^{3/2}\zeta^{5/4}}{12\cdot 5^{-3/8}} e^{-14i\phi}\partial_Z \,, \tag{A.56}$$

with

$$a_{\zeta\gamma} := \frac{f(r)}{1+\gamma^{1/2}\zeta^{3/4}5^{-3/8}\psi^{5/4}Y^{15}} \,. \tag{A.57}$$

Then, we have

$$D_{v_{\zeta\gamma}} W|_{C_\zeta^\gamma} = f(r) + \psi^{5/4} r^{14} > 0 \,, \tag{A.58}$$

such that the tubes $T_\epsilon^{\zeta\gamma}$ are well defined and locally parameterized by

$$T = -1 + \tilde{\epsilon} a \,,\ X = -Z = \frac{1}{\sqrt{5^{1/12}\psi^{1/6}}} - \frac{\gamma^{3/2}\zeta^{5/4}}{12\cdot 5^{-3/8}} e^{-14i\phi}\tilde{\epsilon} \,, \tag{A.59}$$

where $\tilde{\epsilon} = e^{i\chi}\epsilon$.

Let us now consider the forms ω_i: Going to the chart U_1 and restricting to $Y' = i5^{-1/2}X'^5$, we directly infer that $\omega_i = 0$ for $i \notin \{3,5\}$ and that

$$\omega_3 = -dT' \wedge dY' \wedge dZ' \,,\ \omega_5 = -dT' \wedge dX' \wedge dZ' \,. \tag{A.60}$$

Thus,

$$w_5 = -i5^{-1/2}X'^{-4} w_3 = -dT' \wedge dX' \wedge dZ' \,. \tag{A.61}$$

Changing to the coordinates (A.54) then yields

$$dT' \wedge dX' \wedge dZ' = i\gamma^{1/2}\zeta^{1/4} 6\cdot 5^{1/24}\psi^{1/12}(X+Y+Z)(1+5^{1/24}\psi^{1/12}(Y+Z))^2 dT\wedge dX\wedge dZ \,. \tag{A.62}$$

Further,

$$dT\wedge dX\wedge dZ|_{T_\epsilon^{\zeta\gamma}} = -\frac{7}{6}5^{3/8}\gamma^{3/2}\zeta^{5/4} a e^{-13i\phi}\tilde{\epsilon}^2 \left(1 - \frac{r f'(r)}{14 f(r)}\right) dr\wedge d\phi\wedge d\chi \,. \tag{A.63}$$

Hence,

$$w_5|_{T_\epsilon^{\zeta\gamma}} = i7\cdot 5^{3/24}\psi^{1/12} a e^{-13i\phi} Y (1+5^{1/24}\psi^{1/12}(Y+Z))^2 \left(1 - \frac{r f'(r)}{14 f(r)}\right)\tilde{\epsilon}^2 dr\wedge d\phi\wedge d\chi,$$
$$w_3|_{T_\epsilon^{\zeta\gamma}} = 7\cdot 5^{15/24}\psi^{1/12} a e^{-13i\phi} Y^9 (1+5^{1/24}\psi^{1/12}(Y+Z))^2 \left(1 - \frac{r f'(r)}{14 f(r)}\right)\tilde{\epsilon}^2 dr\wedge d\phi\wedge d\chi. \tag{A.64}$$

After performing the explicit integration, we infer that we obtain contributions from the following terms occurring in $\tilde{\beta}^{(10)}$:

$$\begin{aligned}\int_{T_\epsilon^{\zeta\gamma}} \frac{6\psi^6 x_1^7 x_2^7 x_3^7 x_4^2 x_5^2 \omega_5}{W^4} &= \zeta \frac{2}{5}\sqrt{5}\pi^2\psi^3\,,\\ \int_{T_\epsilon^{\zeta\gamma}} \frac{14\psi^5 x_1^6 x_2^6 x_3^6 x_4 x_5 \omega_5}{W^3} &= -\zeta \frac{7}{5}\sqrt{5}\pi^2\psi^3\,,\\ \int_{T_\epsilon^{\zeta\gamma}} \frac{13\psi^4 x_1^5 x_2^5 x_3^5 \omega_5}{W^2} &= \zeta \frac{13}{5}\sqrt{5}\pi^2\psi^3\,,\end{aligned} \tag{A.65}$$

where we have included an additional normalization factor of 10^{-1}.

With similar computations as above one can show that for chart U_2 (which includes p_2) no contribution arises.

Summing the contributions given in (A.65), we infer

$$\int_{T_\epsilon(C_\zeta^\gamma; p_1^\zeta)} \tilde{\beta} = \zeta \frac{8}{5}\sqrt{5}\pi^2\psi^3\ . \tag{A.66}$$

It remains to show that the underlying assumption is correct: We have

$$n_{\zeta\gamma} = \gamma^{-1}\zeta^{-1/2}\frac{1}{4}5^{-1/4}\psi^{-3/2}\frac{x_4^2}{x_3}\left(\partial_3 - i5^{1/2}x_3^4\partial_5\right)\ . \tag{A.67}$$

Hence,

$$n_{\zeta\gamma}\omega = \gamma^{-1}\zeta^{-1/2}\frac{1}{4}5^{-1/4}\psi^{-3/2}\frac{x_4^2}{x_3}\left(\omega_3 - i5^{1/2}x_3^4\omega_5\right) = 0\,, \tag{A.68}$$

where we used (A.61).

References

[1] J. Walcher, *Opening mirror symmetry on the quintic*, *Commun. Math. Phys.* **276** (2007) 671 [hep-th/0605162].

[2] D.R. Morrison and J. Walcher, *D-branes and normal functions*, arXiv:0709.4028.

[3] D.R. Morrison, *Picard-Fuchs equations and mirror maps for hypersurfaces*, hep-th/9111025.

[4] A. Klemm and S. Theisen, *Considerations of one modulus Calabi-Yau compactifications: Picard-Fuchs equations, Kähler potentials and mirror maps*, *Nucl. Phys.* **B 389** (1993) 153 [hep-th/9205041].

[5] A. Font, *Periods and duality symmetries in Calabi-Yau compactifications*, *Nucl. Phys.* **B 391** (1993) 358 [hep-th/9203084].

[6] P. Candelas, X.C. De La Ossa, P.S. Green and L. Parkes, *A pair of Calabi-Yau manifolds as an exactly soluble superconformal theory*, *Nucl. Phys.* **B 359** (1991) 21.

[7] J. Walcher, *Stability of Landau-Ginzburg branes*, *J. Math. Phys.* **46** (2005) 082305 [hep-th/0412274].

[8] I. Brunner, K. Hori, K. Hosomichi and J. Walcher, *Orientifolds of Gepner models*, *JHEP* **02** (2007) 001 [hep-th/0401137].

JHEP09(2008)031

[9] M. Aganagic and C. Vafa, *Mirror symmetry, D-branes and counting holomorphic discs*, hep-th/0012041.

[10] M. Aganagic, A. Klemm and C. Vafa, *Disk instantons, mirror symmetry and the duality web*, *Z. Naturforsch.* **A57** (2002) 1 [hep-th/0105045].

[11] W. Lerche, P. Mayr and N. Warner, *Holomorphic $N = 1$ special geometry of open-closed type-II strings*, hep-th/0207259; *$N = 1$ special geometry, mixed Hodge variations and toric geometry*, hep-th/0208039.

[12] H. Ooguri and C. Vafa, *Knot invariants and topological strings*, *Nucl. Phys.* **B 577** (2000) 419 [hep-th/9912123].

[13] J. Walcher, *Extended holomorphic anomaly and loop amplitudes in open topological string*, arXiv:0705.4098.

[14] J. Walcher, *Evidence for tadpole cancellation in the topological string*, arXiv:0712.2775.

[15] M. Bershadsky, S. Cecotti, H. Ooguri and C. Vafa, *Holomorphic anomalies in topological field theories*, *Nucl. Phys.* **B 405** (1993) 279 [hep-th/9302103].

[16] M. Bershadsky, S. Cecotti, H. Ooguri and C. Vafa, *Kodaira-Spencer theory of gravity and exact results for quantum string amplitudes*, *Commun. Math. Phys.* **165** (1994) 311 [hep-th/9309140].

[17] R. Roiban, C. Romelsberger and J. Walcher, *Discrete torsion in singular G_2-manifolds and real LG*, *Adv. Theor. Math. Phys.* **6** (2003) 207 [hep-th/0203272].

[18] S. Kachru, S.H. Katz, A.E. Lawrence and J. McGreevy, *Open string instantons and superpotentials*, *Phys. Rev.* **D 62** (2000) 026001 [hep-th/9912151].

[19] K. Fukaya, Y.-G. Oh, H. Ohta and K. Ono, *Lagrangian intersection Floer theory-anomaly and obstruction*, http://www.math.kyoto-u.ac.jp/∼fukaya/fooo.dvi, preprint (2000).

[20] J. Walcher, unpublished.

[21] A. Recknagel and V. Schomerus, *D-branes in Gepner models*, *Nucl. Phys.* **B 531** (1998) 185 [hep-th/9712186].

[22] I. Brunner and V. Schomerus, *D-branes at singular curves of Calabi-Yau compactifications*, *JHEP* **04** (2000) 020 [hep-th/0001132].

[23] J. Fuchs, C. Schweigert and J. Walcher, *Projections in string theory and boundary states for Gepner models*, *Nucl. Phys.* **B 588** (2000) 110 [hep-th/0003298].

[24] K. Hori and J. Walcher, *D-branes from matrix factorizations*, talk at *Strings '*04, June 28–July 2 Paris, France 2004, *Comptes Rendus Physique* **5** (2004) 1061 [hep-th/0409204].

[25] D. Orlov, *Derived categories of coherent sheaves and triangulated categories of singularities*, math.AG/0503632.

[26] M. Herbst, K. Hori and D. Page, *Phases of $N = 2$ theories in $1 + 1$ dimensions with boundary*, arXiv:0803.2045.

[27] P.L.H. Cook, H. Ooguri and J. Yang, *New anomalies in topological string theory*, arXiv:0804.1120.

[28] J.M.F. Labastida, M. Mariño and C. Vafa, *Knots, links and branes at large-N*, *JHEP* **11** (2000) 007 [hep-th/0010102].

JHEP09(2008)031

[29] M.-x. Huang, A. Klemm and S. Quackenbush, *Topological string theory on compact Calabi-Yau: modularity and boundary conditions*, hep-th/0612125.

[30] R. Pandharipande, J. Solomon and J. Walcher, *Disk enumeration on the quintic* 3*-fold*, math.SG/0610901, submitted to *J. Am. Math. Soc.* (2008).

[31] J.P. Solomon, *Intersection theory on the moduli space of holomorphic curves with Lagrangian boundary conditions*, math.SG/0606429.